Copper(I)/Dioxygen Reactivity of Mononuclear Complexes with Pyridyl and Quinolyl Tripodal Tetradentate Ligands: Reversible Formation of Cu:O_2 = 1:1 and 2:1 Adducts

Ning Wei,† Narasimha N. Murthy,† Qin Chen,‡ Jon Zubieta,‡ and Kenneth D. Karlin*,†

Departments of Chemistry, The Johns Hopkins University, Baltimore, Maryland 21218, and Syracuse University, Syracuse, New York 13244

Received January 14, 1994®

Copper(I) complexes possessing a series of related tripodal tetradentate ligands with pyridyl- and/or quinolyl-containing groups have been investigated in reactions with dioxygen (O_2). The ligand variations allow for the testing of effects of ligand donor ability and steric factors. Copper–dioxygen complex stabilities, preference for formation of 1:1 Cu–O_2 and/or 2:1 Cu_2–O_2 adducts, Cu_n–O_2 (n = 1, 2), spectroscopic properties, and reactivity characteristics have been investigated. The ligands are L = tris(2-pyridylmethyl)amine (TMPA), bis(2-pyridylmethyl)(2-quinolylmethyl)amine (BPQA), bis(2-quinolylmethyl)(2-pyridylmethyl)amine (BQPA), and tris(2-quinolylmethyl)-amine (TMQA). The 2:1 adduct $[\{(TMPA)Cu\}_2(O_2)]^{2+}$ (**1c**), with a *trans*-(μ-1,2-peroxo)dicopper(II) structure, has previously been shown to form reversibly from the interaction of O_2 with the copper(I) complex $[(TMPA)Cu(RCN)]^+$ (**1a**) (R = Me, Et) (Tyklár, Z.; et al. *J. Am. Chem. Soc.* **1993**, *115*, 2677). The corresponding Cu(I) complexes $[(BPQA)Cu]^+$ (**2a**), $[(BQPA)Cu]^+$ (**3a**), and $[(TMQA)Cu]^+$ (**4a**) have been synthesized as either PF_6^- or ClO_4^- salts. They lack an RCN nitrile ligand as isolated solids, but **2a**–**4a** appear to coordinate nitriles in MeCN or EtCN solutions. The X-ray structure of **4a** has been determined (triclinic space group $P\bar{1}$; a = 13.130 (2), b = 16.570 (2), c = 12.956 (2) Å, α = 111.44 (1) β = 98.49 (1), γ = 84.46 (1)°; V = 2592.1 (6) Å^3; Z = 2), and it exhibits a pseudotetrahedral coordination to the alkylamine and three quinolyl N-donors. Copper(I) complexes **2a** and **3a** react with triphenylphosphine to form adducts $[LCu(PPh_3)]^+$ (**2d**, **3d**). The X-ray structure of **3d** (monoclinic space group $C2/c$; a = 16.341 (4), b = 19.017 (6), c = 26.860 (7) Å; β = 105.48 (2)°, V = 8044 (4) Å^3; Z = 8) indicates that one of the quinolyl arms of the BQPA ligand is uncoordinated and dangles away from the Cu(I) ion, leaving a distorted tetrahedral coordination, comprising $N_{pyridyl}$, $N_{quinolyl}$, $N_{alkylamino}$, and P copper ligation. Cyclic voltammetric measurements carried out on **1a**–**4a** plus $[(TMPA')Cu(CH_3CN)]^+$ (**1a'**; TMPA' possesses a –C(O)Me ester group attached to the 5-position of one pyridyl ring of TMPA) show that the Cu(II)/Cu(I) redox potentials can be greatly influenced by these ligand variations. $E_{1/2}$ values span a large range, from –0.61 to –0.24 V for **1a**–**4a**, versus $Ag/AgNO_3$ in dimethylformamide; the value for **1a'** is –0.56 V. The BPQA complex **2a** reacts rapidly with O_2 at –80 °C in EtCN solvent to give an intensely purple stable solution adduct $[\{(BPQA)Cu\}_2(O_2)]^{2+}$ (**2c**), as evidenced by manometric O_2-uptake measurements (Cu:O_2 = 2:1) and the UV–vis spectrum, which closely resembles that of **1c**, with λ_{max} = 535 (ϵ = 10 500 M^{-1} cm^{-1}), ca. 440 (sh, ϵ = 2000 M^{-1} cm^{-1}), and ca. 600 nm (sh, ϵ = 7600 M^{-1} cm^{-1}). The chemical reactivity parallels that of **1c**; reaction with PPh_3 gives **2d** with evolution of O_2, while exposure to H^+ produces hydrogen peroxide in 94% yield, as determined by iodometric titration. The BQPA-containing complex **3a** reacts to form a dark brown adduct $[(BQPA)Cu(O_2)]^+$ (**3b**), which is stable at –80 °C in EtCN. Manometry (Cu:O_2 = 1:1) and the drastically different UV–vis characteristics with λ_{max} = 378 nm (ϵ = 8200 M^{-1} cm^{-1}) attest to its formulation as a 1:1 adduct, formally a Cu(II)–superoxide species. Reactions of **3b** with PPh_3 and H^+ proceed with formation of products analogous to those found with **2c**, and phosphine adduct **3d** could be isolated. Reaction of **3b** with the TMPA results in a ligand-exchange reaction, with production of peroxo species **1c**, as followed by UV–vis spectroscopy at –80 °C. The binding of O_2 to **3a** to give 1:1 adduct **3b** is reversible, as demonstrated by cycling experiments, i.e., the alternate and repetitive removal of O_2 from **3b** by application of a vacuum, followed by reoxygenation of **3a**; this process was monitored spectrophotometrically. Steric factors are seen to be important in this unique stabilization of the Cu–O_2 complex **3b**. With the even more bulky TMQA ligand complex **4a**, no reaction with O_2 is observed. Possible structures of the Cu-bound O_2 ligand in 1:1 adduct **3b** are enumerated. Dioxygen binding characteristics and variations observed for **1a**–**4a** and **1a'** are examined in terms of electronic (i.e. redox) characteristics and steric effects and in light of recent complete kinetic–thermodynamic characterization of the O_2-binding in **1a**–**3a** (Karlin, K. D.; et al. *J. Am. Chem. Soc.* **1993**, *115*, 9506). Steric and not electronic effects appear to predominate in determining the O_2-reaction chemistry. The biological relevance of 2:1 and 1:1 Cu:O_2 adduct chemistry is also mentioned.

Introduction

The chemistry of copper dioxygen complexes has advanced considerably in the last 10 years.[1-4] Appropriate ligand design and use of low-temperature synthesis, handling, and characterization of Cu_n–O_2 (n = 1, 2) entities have provided insight into the kinetics and thermodynamics of their formation,[5-7] possible structures (i.e. O_2-binding modes), associated spectroscopy,[8-14]

* To whom correspondence should be addressed.
† The Johns Hopkins University.
‡ Syracuse University.
® Abstract published in *Advance ACS Abstracts*, April 1, 1994.
(1) *Bioinorganic Chemistry of Copper*; Karlin, K. D.; Tyeklár, Z., Eds.; Chapman & Hall: New York, 1993.
(2) Karlin, K. D., Tyeklár, Z.; Zuberbühler, A. D. In *Bioinorganic Catalysis*; Reedijk, J., Ed.; Marcel Dekker: New York, 1993; pp 261–315.
(3) Kitajima, N. *Adv. Inorg. Chem.* **1992**, *39*, 1–77.
(4) Sorrell, T. N. *Tetrahedron* **1989**, *45*, 3–68.
(5) Cruse, R. W.; Kaderli, S.; Karlin, K. D.; Zuberbühler, A. D. *J. Am. Chem. Soc.* **1988**, *110*, 6882–6883.
(6) Karlin, K. D.; Wei, N.; Jung, B.; Kaderli, S.; Zuberbühler, A. D. *J. Am. Chem. Soc.* **1991**, *113*, 5868–5870.
(7) Karlin, K. D.; Wei, N.; Jung, B.; Kaderli, S.; Niklaus, P.; Zuberbühler, A. D. *J. Am. Chem. Soc.* **1993**, 9506–9514.

0020-1669/94/1333-1953$04.50/0

Chart 1

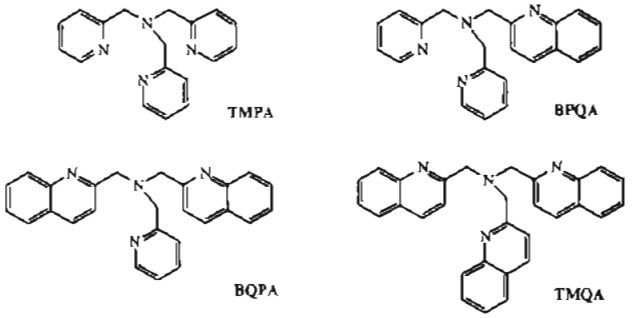

and chemical reactivity, including reversible O_2-binding.[15-18] Nevertheless, relevant aspects of copper(I)/O_2-binding have lagged behind the development of Fe–O_2 chemistry involving heme proteins and model porphyrin–iron complexes,[19-24] in spite of the fact that copper-mediated oxidations are important in a variety of synthetic, industrial, and biological processes.[25-28]

Cu_2–O_2 (2:1) adducts derived from Cu(I) and dioxygen are important in several protein active sites when they are in their oxygenated forms, including hemocyanin (Hc; dioxygen transport protein)[29-31] and tyrosinase (Tyr; *o*-phenol hydroxylase).[30-34] Hemocyanin contains a dinuclear copper center where each copper ion is bound to three imidazole ligands derived from side-chain histidines.[29] Deoxy-Hc, i.e., the reduced dicopper(I) proteins, reacts reversibly with O_2 by a two-electron oxidative addition reaction to generate a bridged peroxo dicopper(II) oxy-Hc (Cu(II)···Cu(II) = 3.55 Å, ν_{O-O} ~750 cm^{-1}).[35]

Biophysical and inorganic chemical interest in the copper–dioxygen binding configuration in oxy-Hc greatly stimulated investigations of Cu/O_2 reactivity and spectroscopic properties of well-defined model complexes. Currently, there are two discrete Cu_2–O_2^{2+} complexes which have been characterized by X-ray crystallography:[8-11,13]

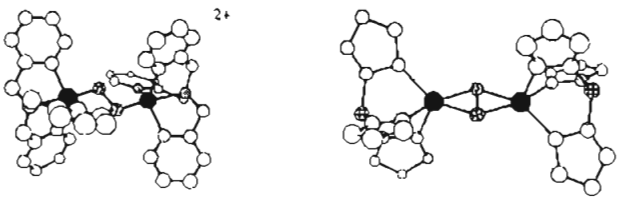

$[\{(TMPA)Cu\}_2(O_2)]^{2+}$ (**1c**) $\{Cu[HB(3,5\text{-}iPr_2pz)_3]\}_2(O_2)$

$[\{(TMPA)Cu\}_2(O_2)]^{2+}$ (**1c**) forms from the reversible reaction of O_2 with $[(TMPA)Cu(RCN)]^+$ (**1a**); this chemical system utilizes the tripodal tetradentate ligand TMPA, tris(2-pyridylmethyl)amine (Chart 1), and **1c** possesses a *trans*-(μ-1,2-O_2)-Cu_2^{2+} moiety.[8,9] The other complex comes from the elegant studies of Kitajima and co-workers,[11,36] who synthesized a Cu_2–O_2 species with a (μ-η^2:η^2-peroxo)dicopper(II) configuration, $\{Cu[HB(3,5\text{-}iPr_2pz)_3]\}_2(O_2)$, where $(HB(3,5\text{-}iPr_2pz)_3$ = hydrotris(3,5-diisopropylpyrazolyl)borate anion). The structural and physical properties of this species revealed that the copper–dioxygen binding in oxy-Hc must involve a similar coordination; this has been confirmed in a recent X-ray structural study on *Limulus polyphemus* oxy-Hc.[37,38]

Cu–O_2 (1:1) adducts are also of interest, since they can serve as precursors for 2:1 adducts, via further reaction of Cu–O_2 with copper(I). Furthermore, recent studies have revealed the presence of such entities as important intermediates involved in the chemistry of several other copper protein active sites, such as dopamine β-hydroxylase,[39] phenylalanine hydroxylase,[40] and amine oxidases.[41] So far, no X-ray structure is available for a 1:1 CuO_2 species. However, chemical/spectroscopic studies have revealed evidence for a number of Cu–O_2 1:1 species, generated either from copper(I)/O_2 reactions[6,7,42-44] or by addition of the superoxide anion (O_2^-) to copper(II) complexes.[45-50] A relevant biological function is carried out by the Cu/Zn enzyme superoxide dismutase (SOD), thought to operate via alternating reactions (i) $Cu(II) + O_2^- \rightarrow Cu(I) + O_2$ and (ii) $Cu(I) + O_2^- + 2H^+ \rightarrow Cu(II) + H_2O_2$, thus effecting the net reaction $2O_2^- + 2H^+ \rightarrow O_2 + H_2O_2$.[51,52] As is pertinent here, a stopped-flow kinetics study[7] indicated that the formation of the dinuclear complex $[\{(TMPA)Cu\}_2(O_2)]^{2+}$ (**1c**) proceeds via the formation of a transient intermediate 1:1 adduct $[(TMPA)Cu(O_2)]^+$ (**1b**).

(8) Jacobson, R. R.; Tyeklár, Z.; Karlin, K. D.; Liu, S.; Zubieta, J. *J. Am. Chem. Soc.* **1988**, *110*, 3690–3692.
(9) Tyeklár, Z.; Jacobson, R. R.; Wei, N.; Murthy, N. N.; Zubieta, J.; Karlin, K. D. *J. Am. Chem. Soc.* **1993**, *115*, 2677–2689.
(10) Kitajima, N.; Fujisawa, K.; Moro-oka, Y.; Toriumi, K. *J. Am. Chem. Soc.* **1989**, *111*, 8975–8976.
(11) Kitajima, N.; Fujisawa, K.; Fujimoto, C.; Moro-oka, Y.; Hashimoto, S.; Kitagawa, T.; Toriumi, K.; Tatsumi, K.; Nakamura, A. *J. Am. Chem. Soc.* **1992**, *114*, 1277–1291.
(12) Pate, J. E.; Cruse, R. W.; Karlin, K. D.; Solomon, E. I. *J. Am. Chem. Soc.* **1987**, *109*, 2624–2630.
(13) Baldwin, M. J.; Ross, P. K.; Pate, J. E.; Tyeklár, Z.; Karlin, K. D.; Solomon, E. I. *J. Am. Chem. Soc.* **1991**, *113*, 8671–8679.
(14) Baldwin, M. J.; Root, D. E.; Pate, J. E.; Fujisawa, K.; Kitajima, N.; Solomon, E. I. *J. Am. Chem. Soc.* **1992**, *114*, 10421–10431.
(15) Paul, P. P.; Tyeklár, Z.; Jacobson, R. R.; Karlin, K. D. *J. Am. Chem. Soc.* **1991**, *113*, 5322–5332.
(16) Nasir, M. S.; Cohen, B. I.; Karlin, K. D. *J. Am. Chem. Soc.* **1992**, *114*, 2482–2494.
(17) Kitajima, N.; Koda, T.; Iwata, Y.; Moro-oka, Y. *J. Am. Chem. Soc.* **1990**, *112*, 8833–8839.
(18) Karlin, K. D.; Tyeklár, Z. In *Bioinorganic Chemistry of Copper*; Karlin, K. D.; Tyeklár, Z., Eds.; Chapman & Hall: New York, 1993; pp 277–291.
(19) Poulos, T. L. *FASEB J.* **1992**, *6*, 674–679.
(20) Watanabe, Y.; Groves, J. T. In *Mechanisms of Catalysis*; Sigman, D. S., Ed.; Academic Press: San Diego, CA, 1992; pp 405–452.
(21) Gunter, M. J.; Turner, P. *Coord. Chem. Rev.* **1991**, *108*, 115–161.
(22) Ostovic, D.; Bruice, T. C. *Acc. Chem. Res.* **1992**, *25*, 314–320.
(23) Meunier, B. *Chem. Rev.* **1992**, *92*, 1411–1456.
(24) Dawson, J. H. *Science* **1988**, *240*, 433–439.
(25) Gubelmann, M. H.; Williams, A. F. *Struct. Bonding (Berlin)* **1983**, *55*, 1–65.
(26) *Oxygen Complexes and Oxygen Activation by Transition Metals*; Martell, A. E., Sawyer, D. T., Eds.; Plenum: New York, 1988.
(27) *Dioxygen Activation and Homogeneous Catalytic Oxidation*; Simándi, L. I., Ed.; Elsevier Science Publishers: Amsterdam, 1991; Vol. 66.
(28) Sheldon, R. A.; Kochi, J. M. *Metal-Catalyzed Oxidations of Organic Compounds*; Academic Press: New York, 1981.
(29) Volbeda, A.; Hol, W. G. J. *J. Mol. Biol.* **1989**, *209*, 249–279.
(30) Solomon, E. I.; Baldwin, M. J.; Lowery, M. D. *Chem. Rev.* **1992**, *92*, 521–542.
(31) Solomon, E. I.; Lowery, M. D. *Science* **1993**, *259*, 1575.
(32) Wilcox, D. E.; Porras, A. G.; Hwang, Y. T.; Lerch, K.; Winkler, M. E.; Solomon, E. I. *J. Am. Chem. Soc.* **1985**, *107*, 4015–4027.
(33) Robb, D. A. In *Copper Proteins and Copper Enzymes*; Lontie, R., Ed.; CRC: Boca Raton, FL, 1984; Vol. 2, pp 207–241.
(34) Lerch, K. *Met. Ions Biol. Syst.* **1981**, *13*, 143–186.
(35) Freedman, T. B.; Loehr, J. S.; Loehr, T. M. *J. Am. Chem. Soc.* **1976**, *98*, 2809–2815.
(36) Kitajima, N.; Fujisawa, K.; Moro-oka, Y.; Toriumi, K. *J. Am. Chem. Soc.* **1989**, *111*, 8975–8976.
(37) Magnus, K.; Ton-That, H. *J. Inorg. Biochem.* **1992**, *47*, 20.
(38) Karlin, K. D. *Science* **1993**, *261*, 701–708.
(39) Brenner, M. C.; Klinman, J. P. *Biochemistry* **1989**, *28*, 4664–4670.
(40) Pember, S. O.; Johnson, K. A.; Villafranca, J. J.; Benkovic, S. J. *Biochemistry* **1989**, *28*, 2124–2130.
(41) Dooley, D. M.; McGuirl, M. A.; Brown, D. E.; Turowski, P. N.; McIntire, W. S.; Knowles, P. F. *Nature* **1991**, *349*, 262–264.
(42) Thompson, J. S. *J. Am. Chem. Soc.* **1984**, *106*, 4057–4059.
(43) Thompson, J. S. In *Biological & Inorganic Copper Chemistry*; Karlin, K. D., Zubieta, J., Eds.; Adenine Press: Guilderland, NY, 1986; Vol. 2, pp 1–10.
(44) Tahir, M. M.; Karlin, K. D. *J. Am. Chem. Soc.* **1992**, *114*, 7600–7601.
(45) Nappa, M.; Valentine, J. S.; Miksztal, A. R.; Schugar, H. G.; Isied, S. S. *J. Am. Chem. Soc.* **1979**, *101*, 7744–7746.
(46) O'Young, C.-L.; Lippard, S. J. *J. Am. Chem. Soc.* **1980**, *102*, 4920–4924.
(47) Nichida, Y.; Unoura, K.; Watanabe, I.; Yokomizo, T.; Kato, Y. *Inorg. Chim. Acta* **1991**, *181*, 141–143.
(48) Cabelli, D. E.; Bielski, B. H. J. *Holcman, J. J. Am. Chem. Soc.* **1987**, *109*, 3665–3669.
(49) Bailey, C. L.; Bereman, R. D.; Rillema, D. P. *Inorg. Chem.* **1986**, *25*, 3149–3153.
(50) Weinstein, J.; Bielski, B. H. J. *J. Am. Chem. Soc.* **1980**, *102*, 4916–4919.

Scheme 1

$$n\,[LCu]^+ \underset{EtCN}{\overset{O_2,\ -80^\circ C}{\rightleftharpoons}} [(LCu)_nO_2]^{n+}$$

$n = 1$ or 2

	[(TMPA)Cu(RCN)]$^+$	[(BPQA)Cu]$^+$	[(BQPA)Cu]$^+$	[(TMQA)Cu]$^+$
	1a	**2a**	**3a**	**4a**
$[(LCu)O_2]^+$	**1b**	**2b**	**3b**	
$[(LCu)_2O_2]^{2+}$	**1c**	**2c**	**3c**	

With the success in utilizing TMPA as a ligand for the copper ion, we have been interested to alter this tripodal tetradentate donor, in order to elucidate those factors which are important in influencing the formation and stability of resulting copper–dioxygen complexes. Such modifications include changes in chelating ring size in these N4 tetradentate pyridine–amine tripodal ligands.[53] In this report, the variations being examined are those coming about as a consequence of substituting quinolyl for pyridyl donors, i.e. L = BPQA (bis(2-pyridylmethyl)(2-quinolylmethyl)amine), L = BQPA (bis(2-quinolylmethyl)(2-pyridylmethyl)amine), and L = TMQA (tris(2-quinolylmethyl)-amine (Chart 1). These tetradentate tripodal ligands may be used to vary the number of the bulkier and more hydrophobic quinolyl groups and test the consequences of variations in (i) ligand electron donation effects and (ii) ligand steric effects. Our expectations were that some or all of the quinolyl-containing ligands might provide increased thermal stability to the resulting copper–dioxygen adducts, perhaps even stabilizing a 1:1 adduct $[LCu(O_2)]^+$, due to a steric hindrance effect.

In fact, some of these expectations are realized, as detailed in this present chemical/spectroscopic study; a complementary kinetics/thermodynamics investigation is described elsewhere.[7] In this report, the synthesis and characterization of new mononuclear copper(I) complexes $[LCu]^+$ (**2a–4a**) are described, including the X-ray structure of $[(TMQA)Cu]^+$ and a phosphine Cu(I) adduct $[(BPQA)Cu(PPh_3)]^+$. Since reaction of O_2 with copper(I) complexes involved redox chemistry, the electrochemistry of complexes **1a–4a** is also described. The reactions of complexes **2a** and **3a** with O_2 at low temperature (–80 °C) are also detailed. We find that these quinolyl ligands very much influence the dioxygen chemistry of copper(I) complexes and that 1:1 or 2:1 adducts can be separately stabilized (Scheme 1).

Results and Discussion

Synthesis of Cu(I) Complexes. Copper(I) complexes **1a–4a** are prepared by adding 1 equiv of appropriate tripodal ligand and $[Cu(CH_3CN)_4]Y$ (Y = PF_6^-, ClO_4^-) under argon in organonitrile solution. The synthesis and handling/study of these Cu(I) complexes (**1a–3a**) are carried out exclusively in organonitrile solvents. In CH_2Cl_2, all cuprous $[LCu]^+$ complexes, except for the L = TMQA complex (i.e., **4a**), react rapidly with dichloromethane solvent by abstracting chlorine, producing chloride Cu(II) $[LCu(Cl)]^+$ adducts.[54] Copper(I) triphenylphosphine complexes were prepared by reacting either 1 equiv of PPh_3 with $[LCu]^+$ in acetonitrile at room temperature or 2 equivalents of PPh_3 with $[(LCu)_nO_2]^{n+}$ (n = 1, 2) at low temperature in propionitrile solvent (vide infra).

$$[Cu(CH_3CN)_4]Y + L\ (\text{Tripodal Ligands}) \longrightarrow [LCu]Y$$

(Y = PF_6^- or ClO_4^-)

1a L=TMPA
2a L=BPQA
3a L=BQPA
4a L=TMQA

$$[LCu]Y + PPh_3 \longrightarrow [LCu(PPh_3)]Y$$

(Y = PF_6^- or ClO_4^-)

2d L = BPQA
3d L = BQPA

From C, H, N combustion analysis, ^{1}H NMR spectroscopy, and X-ray structural studies on $[(TMQA)Cu]ClO_4$ (vide infra), we find that none of the isolated solid Cu(I) complexes possessing at least one quinolyl donor group contain an additional coordinated nitrile ligand. However, copper(I) complexes with the TMPA ligand, as well as the TMPA′ ligand (where TMPA′ possesses a –C(O)Me ester group attached to the 5-position of one pyridine ring of TMPA), do have and apparently require a nitrile ligand for the completion of the coordination sphere.[9,53] The Cu(I) coordination center of $[(TMPA')Cu(CH_3CN)]^+$ was determined crystallographically[9] and is depicted in the following drawing:

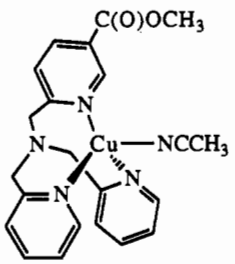

$[(TMPA')Cu(CH_3CN)]^+$

The difference in requirement for an additional nitrile ligand between TMPA and other tripod-ligand-containing complexes may be due to steric hindrance around the Cu(I) center, derived from the bulky quinolyl donors. However, in RCN solutions, we believe that nitriles serve as coordinating ligands in quinolyl-containing Cu(I) complexes, giving $[LCu(RCN)]^+$ by pushing the equilibrium

$$[LCu]^+ + RCN \rightleftharpoons [LCu(RCN)]^+$$

toward the right. This conclusion is supported by the observed quantitative difference in UV–vis spectra of $[(TMQA)Cu]^+$ in CH_3CN versus CH_2Cl_2. In CH_3CN, the yellow $[(TMQA)Cu]^+$ solution exhibits λ_{max} (ϵ, M^{-1} cm^{-1}) at 304 (8000), 317 (7400), 370 nm (sh, 2400); in CH_2Cl_2, $[TMQA)Cu]^+$ solutions exhibit bands at 305 (5300), 317 (4600), and 380 nm (6800).

Structure of $[(TMQA)Cu]ClO_4$ (4a-ClO_4). X-ray-quality crystals of $[TMQA)Cu]ClO_4$ were obtained by recrystallizing the copper(I) complex from acetonitrile/ether. A summary of crystal and data refinement for (**4a-ClO_4**) is given in Table 1, while atom coordinates and thermal parameters are found in Table 2. Selected bond lengths and angles are provided in Table 3, and an ORTEP diagram is shown in Figure 1.

The structure of **4a** contains of $[(TMQA)Cu]^+$ cations; the unit cell consists of two independent molecules, each with only very slightly different bond lengths and angles. Thus, the following discussion is representative but applies specifically to one of these two molecules. Each Cu(I) moiety possesses ligation to three quinolyl nitrogen atoms and one tertiary amine nitrogen atom in a pseudotetrahedral geometry. Relevant dihedral angles are Cu1–

(51) Lu, Y.; LaCroix, L. B.; Lowery, M. D.; Solomon, E. I.; Bender, C. J.; Peisack, J.; Roe, J. A.; Gralla, E. B.; Valentine, J. S. *J. Am. Chem. Soc.* **1993**, *115*, 5907–5918.
(52) Bertini, I.; Banci, L.; Piccioli, M. *Coord. Chem. Rev.* **1990**, *100*, 67–103.
(53) Jacobson, R. R. Ph.D. Dissertation Thesis, State University of New York at Albany, 1989.
(54) Jacobson, R. R.; Tyeklár, Z.; Karlin, K. D. *Inorg. Chim. Acta* **1991**, *181*, 111–118.

Table 1. Summary of Crystal and Refinement Data for [(TMQA)Cu]ClO_4 (**4a-ClO_4**) and [(BQPA)Cu(PPh_3)]ClO_4 (**3d-ClO_4**)

	4a-ClO_4	**3d-ClO_4**
formula	$C_{60}H_{48}Cu_2Cl_2N_8O_8$	$C_{44}H_{33}CuN_4O_4ClP$
T, K	253	296
MW	1207.08	811.74
crystal system	triclinic	monoclinic
space group	$P\bar{1}$	$C2/c$
a, Å	13.130(2)	16.341(4)
b, Å	16.570(2)	19.017(6)
c, Å	12.956(2)	26.860(7)
α, deg	111.44(1)	90.00
β, deg	98.49(1)	105.48(2)
γ, deg	84.46(1)	90.00
V, Å^3	2592.1(6)	8044(4)
$F(000)$	1240	3344
Z	2	8
D_{calc}, g/cm^3	1.546	1.336
abs coeff, cm^{-1}	9.91	6.92
no. of independent reflns	2544 ($\geq 3\sigma(I)$)	1532 ($\geq 3\sigma(I)$)
largest peak/hole, e Å^{-3}	0.87/−1.12	0.58/−0.49
R^a	0.057	0.095
$R_w{}^b$	0.064	0.105

^{a} $R = \sum[|F_o| - |F_c|/\sum|F_o|$. ^{b} $R_w = [\sum_w(|F_o| - |F_c|)^2/\sum_w|F_o|^2]^{1/2}$; $w = 4F_o^2/\sigma^2(F_o^2)$.

N1–N2/Cu–N3–N4 = 89.24°, Cu1–N1–N3/Cu1–N2–N4 = 88.70°, and Cu1–N1–N4/Cu1–N2–N3 = 92.14°. The Cu1 atom lies 0.245 Å above the N2, N3, N4 plane, toward the N1 atom. The Cu–N_{quin} bond lengths range from 1.97 to 2.03 Å and are very similar to those Cu–N_{py} distances found in typical tetracoordinate Cu(I) complexes (2.0–2.05 Å).[55–57] However, they are longer than those observed in tricoordinated Cu(I) complexes, where Cu–N_{py} distances are typically 1.90–1.94 Å.[55,57] The "harder" amine nitrogen N1 binds more weakly to the Cu(I) ion with a Cu1–N1 distance of 2.186(4) Å. A nice hydrophobic pocket exists opposite the Cu1–N1 vector; additional binding of a ligand in this position would probably be restricted to a small donor such as RCN. Otherwise, binding of a large ligand would most likely result in a severe coordination distortion or loss of a quinolyl donor atom.

Structure of [(BQPA)Cu(PPh_3)]ClO_4 (3d-ClO_4). X-ray-quality crystals of [(BQPA)Cu(PPh_3)]ClO_4 were also obtained by recrystallizing the complex from acetonitrile/ether. Crystal data, refinement parameters, and coordinates with thermal parameters are given in Tables 1 and 4, respectively, while selected bond distances and angles are listed in Table 3. Figure 2 depicts the structure of **3d**, which clearly indicates the PPh_3 coordination and a tetracoordinated Cu(I) ion with a "dangling" uncoordinated quinolyl group. Ligation to Cu(I) occurs through the tertiary amine nitrogen N1, the pyridyl nitrogen N2, and the quinolyl nitrogen N3 of the ligand, plus the phosphorus atom of the PPh_3 molecule. A very similar structure has been observed for the [(TMPA)Cu(PPh_3)]$^+$ complex.[9] In [(BQPA)Cu(PPh_3)]$^+$, the copper atom is displaced 0.172 Å out of the P1, N2, N3 plane toward the tertiary amine nitrogen, forming a distorted tetrahedral coordination environment around Cu(I). The dihedral angles are Cu1–N1–N3/Cu–P1–N2 = 70.66°, Cu1–N1–N2/Cu–P1–N3 = 69.29°, and Cu1–N1–P1/Cu1–N2–N3 = 87.72°. The Cu–P distance (Cu–P = 2.200(9) Å) is similar to the value observed in [(TMPA)Cu(PPh_3)]$^+$ and is also close to those values observed for related structures possessing alkylamino–pyridyl polydentate ligands (Cu–P ~ 2.21 Å).[58–60] The Cu–N1 distance is 2.19 (2) Å, very similar to those of other related complexes, however, shorter than the value (2.25 Å) observed in [(TMPA)-Cu(PPh_3)]$^+$.[9] The Cu–N_{py} distance (Cu–N2 = 2.10 Å) is slightly longer than those in related tetradentate copper complexes (Cu–N_{py} = 1.95–2.04 Å),[60–62] and the same is true for the Cu–N_{quin} distance (Cu–N3 = 2.10 Å); this latter value is slightly greater than those observed in the structure of [(TMQA)Cu]$^+$ (**4a**) (Cu–N_{quin} = 1.97–2.03 Å) (vide supra). The slightly longer distance may result from some steric interaction between the quinolyl ring containing N3 and the phenyl groups of the PPh_3 moiety, which could slightly lengthen the Cu–N_{py} and Cu–N_{quin} bonds.

Electrochemistry. The half-wave potentials for all copper(I) complexes were measured by cyclic voltammetry (CV) under argon in dimethylformamide (DMF) solvent. The results are listed in Table 5. In DMF, all copper(I) complexes displayed a single quasi-reversible one-electron redox behavior with i_{pa}/i_{pc} = 0.80–1.02. Peak separations were all less than 110 mV at a scan rate of 100 mV/s. The ferrocene–ferrocenium couple under the same conditions showed ΔE_p = 89 mV and $E_{1/2}$ = 0.02 V vs $Ag/AgNO_3$. A typical CV scan for [(TMQA)Cu]$^+$ (**4a-ClO_4**) is given in Figure 3. Results from bulk electrolysis correspond to a one-electron process per copper complex; these experiments were accompanied by a color change from yellow (e.g., Cu(I) complex) to blue-green (e.g., oxidized Cu(II) species). The CV of a coulometrically oxidized solution gave the exact complement as that of the original Cu(I) complex solution at the same scan rate.

From Table 5, it is evident that when pyridyl donors of the parent TMPA ligand are replaced by quinolyl donors or when the modified TMPA ligand containing an electron-withdrawing ester substituent (i.e., TMPA; vide supra) is used, the $E_{1/2}$ values of their Cu(I) complexes become more positive, resulting in more thermodynamically stable Cu(I) complexes. Over the series of complexes **1a–4a**, the effect upon $E_{1/2}$ is dramatic (i.e., 0.37-V range) (Table V). These results suggest that TMPA and quinolyl-containing ligands BPQA, BQPA, and TMQA are weaker electron donors than TMPA. Many factors influence the redox potential of copper complexes including (a) ligand topology or complex coordination geometry as imposed by constraining chelating ligands, (b) the types of donor atoms, and (c) ligand substituent effects.[55,57,59,63–66] Here, all Cu(I) complexes are tetracoordinate and the copper(I) ions form five-membered rings with these chelating ligands; the coordination geometries are likely to be very similar in all complexes. So, differences in redox potential resulting from variations in chelate ring size can be precluded; such effects have been shown to be important in other systems.[53,55,57,67] We suggest that the two main contributions to the redox potential differences observed here are (i) ligand basicity and (ii) the effect of local environment and polarity as a result of changes in substituent, i.e. that there is or is not a carbon atom (which is part of the quinolyl benzene group) on the 6-position of a pyridine ring.

Quinoline is a less basic group than pyridine, i.e., a weaker σ donor to the copper ion than pyridine (pK_b = 8.74 for pyridine,

(55) Zubieta, J.; Karlin, K. D., Hayes, J. C. In *Copper Coordination Chemistry: Biochemical and Inorganic Perspectives*; Karlin, K. D., Zubieta, J., Eds.; Adenine Press: Albany, NY, 1983; pp 97–108.
(56) Karlin, K. D., Dahlstrom, P. L.; Hayes, J. C.; Simon, R. A.; Zubieta, J. *Cryst. Struct. Commun.* **1982**, *11*, 907–912.
(57) Karlin, K. D.; Sherman, S. E. *Inorg. Chem. Acta* **1982**, *65*, L39–L40.
(58) Karlin, K. D.; Cruse, R. W.; Gultneh, Y.; Farooq, A.; Hayes, J. C.; Zubieta, J. *J. Am. Chem. Soc.* **1987**, *109*, 2668–2679.
(59) Hathaway, B. J. In *Comprehensive Coordination Chemistry*; Wilkinson, G., Ed.; Pergamon: New York, 1987; Vol. 5, pp 533–774.
(60) Karlin, K. D.; Ghosh, P.; Cruse, R. W.; Farooq, A.; Gultneh, Y.; Jacobson, R. R.; Blackburn, N. J.; Strange, R. W.; Zubieta, J. *J. Am. Chem. Soc.* **1988**, *110*, 6769–6780.
(61) Karlin, K. D.; Haka, M. S.; Cruse, R. W.; Meyer, G. J.; Farooq, A.; Gultneh, Y.; Hayes, J. C.; Zubieta, J. *J. Am. Chem. Soc.* **1988**, *110*, 1196–1207.
(62) Karlin, K. D.; Hayes, J. C.; Hutchinson, J. P.; Hyde, J. R.; Zubieta, J. *Inorg. Chim. Acta* **1982**, *64*, L219–L220.
(63) Miyoshi, K.; Tanaka, H.; Kimura, E.; Tsuboyama, S.; Murata, S.; Shimizu, H.; Ishizu, K. *Inorg. Chim. Acta* **1983**, *78*, 23–30.
(64) Augustin, M. A.; Yandell, J. K.; Addison, A. W.; Karlin, K. D. *Inorg. Chim. Acta* **1981**, *55*, L35.
(65) Patterson, G. S.; Holm, R. H. *Bioinorg. Chem.* **1975**, *4*, 257–275.
(66) Addison, A. W. *Inorg. Chim. Acta* **1989**, *162*,
(67) Karlin, K. D.; Hayes, J. C.; Juen, S.; Hutchinson, J. P.; Zubieta, J. *Inorg. Chem.* **1982**, *21*, 4106–4108.

Table 2. Positional Parameters and B(eq) Values for **4a-ClO$_4$**

atom	x	y	z	B(eq), Å^2	atom	x	y	z	B(eq), Å^2
Cu(1)	0.33395(5)	0.35325(4)	0.61447(5)	2.40(3)	C21	0.3218(4)	0.3281(4)	0.8242(5)	3.4(1)
Cu2	−0.01572(5)	0.14570(4)	0.26327(6)	2.68(3)	C22	0.2135(4)	0.3424(4)	0.7740(5)	2.9(1)
Cl1	0.7417(1)	0.4127(1)	0.8982(1)	3.08(6)	C23	0.1287(5)	0.3410(4)	0.8293(5)	3.8(1)
Cl2	0.4503(1)	0.1553(1)	0.9625(1)	3.90(7)	C24	0.0318(5)	0.3481(4)	0.7807(5)	4.1(1)
O1	0.6988(3)	0.3783(3)	0.9677(3)	3.8(2)	C25	0.0143(4)	0.3609(4)	0.6780(5)	3.3(1)
O2	0.6730(4)	0.4779(3)	0.8774(5)	7.0(3)	C26	−0.0835(5)	0.3725(4)	0.6234(5)	4.2(1)
O3	0.8400(4)	0.4455(4)	0.9473(4)	6.3(3)	C27	−0.0938(5)	0.3901(4)	0.5281(5)	4.2(1)
O4	0.7517(4)	0.3445(4)	0.7931(4)	7.0(3)	C28	−0.0071(5)	0.3949(4)	0.4803(5)	3.6(1)
O5	0.3892(5)	0.2284(4)	1.0180(4)	8.1(3)	C29	0.0902(4)	0.3814(4)	0.5292(5)	3.0(1)
O6	0.4365(8)	0.1376(5)	0.8520(5)	15.6(6)	C30	0.1032(4)	0.3644(3)	0.6279(4)	2.7(1)
O7	0.4185(7)	0.0835(5)	0.9725(9)	15.1(6)	C31	−0.2148(5)	0.1213(4)	0.3269(5)	4.3(1)
O8	0.5469(6)	0.1617(8)	1.003(1)	21.4(7)	C32	−0.1304(4)	0.1267(4)	0.4217(5)	3.3(1)
N1	0.3994(3)	0.3628(3)	0.7835(4)	2.8(2)	C33	−0.1578(5)	0.1214(4)	0.5204(6)	4.6(1)
N2	0.4291(3)	0.2478(3)	0.5684(3)	2.3(2)	C34	−0.0826(5)	0.1151(5)	0.6010(6)	4.9(2)
N3	0.2013(3)	0.3532(3)	0.6759(3)	2.5(2)	C35	0.0208(5)	0.1152(4)	0.5879(5)	3.5(1)
N4	0.3878(3)	0.4726(3)	0.6615(3)	2.2(2)	C36	0.1039(5)	0.1069(4)	0.6669(5)	4.4(1)
N5	−0.1856(3)	0.1435(3)	0.2364(4)	3.1(2)	C37	0.2016(5)	0.1091(4)	0.6515(5)	4.3(1)
N6	−0.0342(3)	0.1315(3)	0.4079(4)	2.8(2)	C38	0.2238(5)	0.1195(4)	0.5540(5)	3.9(1)
N7	−0.0400(3)	0.2524(3)	0.2283(3)	2.4(2)	C39	0.1462(4)	0.1281(4)	0.4764(5)	3.2(1)
N8	−0.0261(3)	0.0237(3)	0.1480(3)	2.7(2)	C40	0.0428(4)	0.1258(3)	0.4905(4)	2.7(1)
C1	0.4146(4)	0.4550(4)	0.8430(5)	3.3(1)	C41	−0.2194(5)	0.2304(4)	0.2391(5)	4.3(1)
C2	0.4242(4)	0.5061(3)	0.7691(4)	2.6(1)	C42	−0.1380(4)	0.2795(4)	0.2170(4)	2.9(1)
C3	0.4645(4)	0.5894(4)	0.8173(5)	3.2(1)	C43	−0.1693(4)	0.3540(4)	0.1901(5)	3.3(1)
C4	0.4631(4)	0.6393(4)	0.7554(5)	3.2(1)	C44	−0.0997(4)	0.3991(4)	0.1718(5)	3.3(1)
C5	0.4237(4)	0.6071(3)	0.6410(4)	2.6(1)	C45	0.0055(4)	0.3718(3)	0.1790(4)	2.7(1)
C6	0.4178(4)	0.6561(4)	0.5704(5)	3.2(1)	C46	0.0838(4)	0.4125(4)	0.1540(5)	3.4(1)
C7	0.3808(4)	0.6201(4)	0.4602(5)	3.4(1)	C47	0.1824(5)	0.3833(4)	0.1631(5)	3.7(1)
C8	0.3492(4)	0.5355(4)	0.4143(5)	3.2(1)	C48	0.2113(4)	0.3136(4)	0.1997(5)	3.3(1)
C9	0.3525(4)	0.4865(3)	0.4811(4)	2.6(1)	C49	0.1374(4)	0.2717(3)	0.2234(4)	2.7(1)
C10	0.3881(4)	0.5226(3)	0.5962(4)	2.2(1)	C50	0.0334(4)	0.2986(3)	0.2106(4)	2.2(1)
C11	0.4947(4)	0.3091(4)	0.7668(5)	3.3(1)	C51	−0.2032(5)	0.0754(4)	0.1266(5)	4.1(1)
C12	0.4903(4)	0.2368(3)	0.6546(4)	2.5(1)	C52	−0.1230(4)	0.0017(4)	0.1097(5)	3.1(1)
C13	0.5557(4)	0.1618(4)	0.6415(5)	3.5(1)	C53	−0.1493(4)	−0.0856(4)	0.0558(5)	3.4(1)
C14	0.5618(4)	0.1012(4)	0.5379(5)	3.6(1)	C54	−0.0746(4)	−0.1493(4)	0.0440(5)	3.5(1)
C15	0.5031(4)	0.1124(4)	0.4437(4)	2.9(1)	C55	0.0292(4)	−0.1288(4)	0.0815(4)	2.9(1)
C16	0.5087(4)	0.0553(4)	0.3327(5)	3.6(1)	C56	0.1122(5)	−0.1916(4)	0.0729(5)	3.6(1)
C17	0.4515(5)	0.0712(4)	0.2461(5)	3.9(1)	C57	0.2096(5)	−0.1675(4)	0.1087(5)	3.9(1)
C18	0.3819(5)	0.1435(4)	0.2657(5)	3.6(1)	C58	0.2322(4)	−0.0797(4)	0.1571(5)	3.6(1)
C19	0.3727(4)	0.1999(4)	0.3719(4)	2.8(1)	C59	0.1537(4)	−0.0167(4)	0.1689(5)	3.1(1)
C20	0.4345(4)	0.1867(3)	0.4630(4)	2.3(1)	C60	0.0510(4)	−0.0401(3)	0.1324(4)	2.6(1)

Table 3. Selected Bond Distances (Å) and Angles (deg) for Cu(I) Complexes

[(TMQA)Cu]ClO$_4$ (**4a-ClO$_4$**)		[(BQPA)Cu(PPh$_3$)]ClO$_4$ (**3d-ClO$_4$**)	
	Bond Distances		
Cu1–N1	2.186(4)	Cu–P1	2.200(9)
Cu1–N2	2.001(4)	Cu–N1	2.19(2)
Cu1–N3	2.020(4)	Cu–N2	2.10(2)
Cu1–N4	2.010(4)	Cu–N3	2.06(3)
Cu2–N5	2.208(4)		
Cu2–N6	2.024(4)		
Cu2–N7	1.967(4)		
Cu2–N8	2.030(4)		
	Bond Angles		
N1–Cu1–N2	83.8(2)	P1–Cu–N1	122(1)
N1–Cu1–N3	81.7(2)	N1–Cu–N2	79(1)
N1–Cu1–N4	83.4(2)	P1–Cu–N2	117.4(9)
N2–Cu1–N3	122.1(2)	N1–Cu–N3	78(1)
N2–Cu1–N4	120.6(2)	P1–Cu–N3	132.6(8)
N3–Cu1–N4	113.0(2)	N2–Cu–N3	108(1)

pK_b = 9.12 for quinoline). Thus, less electron density is provided to a Cu(I) center when a pyridyl donor is replaced by a quinolyl group, making it more difficult to oxidize Cu(I) to Cu(II), i.e., resulting in a more positive $E_{1/2}$ value. The presence of one electron-withdrawing ester group in [(TMPA′)Cu(CH$_3$CN)]$^+$ (**1a′**; vide supra) has only a marginal effect on the observed redox potential (Table 5). James and Williams[68] observed a more significant positive shift in redox potential for 5,5′-(CO$_2$Et)$_2$-2,2-bipy (bipy = 2,2′-bipyridyl) bis(ligand) complexes of copper compared to the parent [Cu(bipy)$_2$]$^{2+/+}$ complexes.

(68) James, B. R.; Williams, R. J. P. *J. Chem. Soc.* **1961**, 2007.

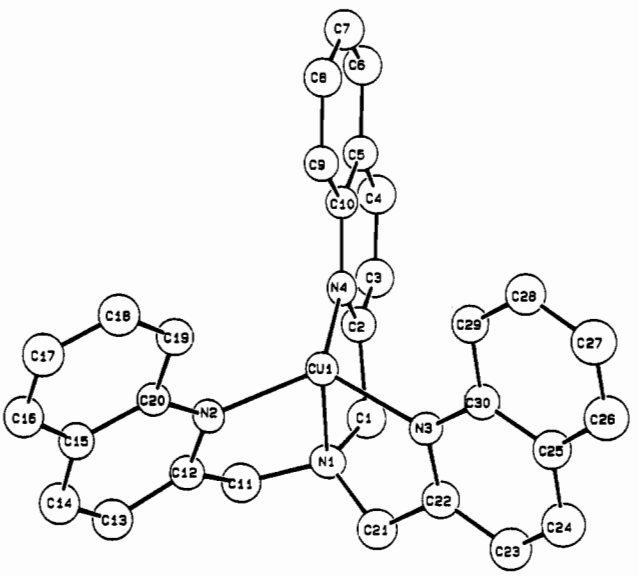

Figure 1. ORTEP diagram of the cationic portion of [(TMQA)Cu]$^+$ (**4a**) showing the satom-labeling scheme.

The increased hydrophobicity of quinolyl ligand donors undoubtedly also helps increase $E_{1/2}$ values, since a lower dielectric environment provided by nonpolar quinolyl species favors lower charges, and thus the Cu(I) (relative to Cu(II)) oxidation state. The redox potential for [6,6′-Me$_2$bipy)$_2$]$^{2+/+}$ is more than 0.5 V more positive than that for [Cu(bipy)$_2$]$^{2+}$.[68] However, this effect is due the methyl substituents enforcing a pseudotetrahedral geometry, favoring Cu(I). Sorrell and Jameson[69] showed that

Table 4. Positional Parameters and $B(eq)$ Values for **3d**-ClO_4

atom	x	y	z	$B(eq)$, Å^2
Cu1	0.4852(2)	0.1461(2)	0.1136(1)	3.8(2)
Cl1	0.260(1)	0.1817(7)	0.6713(6)	10.0(8)
P	0.4855(6)	0.1768(4)	0.0351(3)	3.7(4)
O1	0.310(2)	0.126(2)	0.667(1)	10.8(9)
O2	0.276(2)	0.244(2)	0.653(1)	12(1)
O3	0.192(4)	0.168(3)	0.680(3)	30(3)
O4	0.269(4)	0.196(3)	0.723(2)	23(2)
N1	0.376(2)	0.099(1)	0.133(1)	4(1)
N2	0.456(2)	0.223(2)	0.1599(9)	4(2)
N3	0.539(2)	0.063(1)	0.159(1)	4(2)
N4	0.170(2)	0.144(2)	0.119(1)	8(2)
C1	0.582(2)	0.166(1)	0.015(1)	3(2)
C2	0.579(2)	0.147(2)	–0.038(1)	5(2)
C3	0.661(3)	0.140(2)	–0.050(2)	8(3)
C4	0.739(3)	0.150(2)	–0.007(3)	11(4)
C5	0.730(3)	0.170(2)	0.036(1)	6(2)
C6	0.658(3)	0.173(2)	0.048(1)	5(2)
C7	0.461(3)	0.271(2)	0.026(1)	4(2)
C8	0.385(3)	0.295(2)	0.035(1)	6(2)
C9	0.368(3)	0.365(3)	0.027(2)	8(3)
C10	0.421(5)	0.413(3)	0.017(2)	10(4)
C11	0.495(4)	0.389(3)	0.005(2)	10(3)
C12	0.514(3)	0.317(3)	0.011(2)	8(3)
C13	0.405(2)	0.134(2)	–0.019(1)	4(2)
C14	0.397(2)	0.062(2)	–0.014(1)	5(2)
C15	0.345(3)	0.023(2)	–0.054(2)	9(3)
C16	0.296(2)	0.060(3)	–0.094(2)	6(2)
C17	0.303(3)	0.130(2)	–0.099(1)	7(2)
C18	0.360(2)	0.174(2)	–0.061(1)	6(2)
C21	0.487(3)	0.291(3)	0.159(2)	10(3)
C22	0.456(3)	0.350(4)	0.185(2)	15(5)
C23	0.397(4)	0.330(2)	0.204(2)	9(3)
C24	0.361(2)	0.267(3)	0.208(1)	7(3)
C25	0.392(3)	0.208(2)	0.181(1)	5(2)
C26	0.376(2)	0.128(2)	0.182(1)	5(2)
C31	0.622(3)	0.056(2)	0.184(1)	4(2)
C32	0.677(3)	0.111(2)	0.186(1)	6(2)
C33	0.765(3)	0.108(2)	0.219(1)	6(2)
C34	0.799(3)	0.044(3)	0.240(1)	7(3)
C35	0.744(3)	–0.008(2)	0.240(1)	6(2)
C36	0.655(2)	–0.007(2)	0.212(1)	4(2)
C37	0.591(3)	–0.064(2)	0.207(2)	7(3)
C38	0.510(2)	–0.053(2)	0.184(1)	5(2)
C39	0.487(2)	0.011(2)	0.160(1)	3(2)
C40	0.394(2)	0.025(2)	0.136(2)	7(2)
C41	0.078(6)	0.152(5)	0.131(2)	26(8)
C42	0.07(1)	0.199(7)	0.166(5)	38(2)
C43	–0.031(6)	0.184(5)	0.151(3)	23(3)
C44	–0.049(4)	0.119(4)	0.151(2)	16(2)
C45	–0.015(5)	0.056(3)	0.141(2)	15(2)
C46	0.069(3)	0.081(4)	0.132(2)	10(4)
C47	0.106(3)	0.016(3)	0.116(2)	9(3)
C48	0.183(2)	0.026(2)	0.106(1)	6(2)
C49	0.212(2)	0.093(2)	0.106(1)	6(2)
C50	0.295(2)	0.113(2)	0.093(1)	5(2)

in tripodal Cu(I) complexes $[Cu(trpyn)]^+$ (trpyn = tris[2-(1-pyrazolyl)ethyl]amine) and its 3,5-dimethylpyrazolyl analogue trpynMe$_6$ possessing geometries similar to those of complexes **1a**–**4a**, the redox potential of the latter is ~0.2 V more positive, due to an environmental effect of increased nonpolarity. A *tert*-butyl analogue is still ~0.3 V even more positive.[69] We presume that quinolyl for pyridyl substitution has a similar effect, since the change to nonpolar quinolyl substituent occurs at the carbon adjacent to the "pyridyl" nitrogen donor.

The ease of electrochemical oxidation of these $[LCu]^+$ cuprous complexes correlates in a general way with their O_2 reactivity, as described below and as determined in a separate kinetic study.[7] Complexes **1a**–**3a** do react with O_2 at low temperature, forming copper–dioxygen adducts, which can be characterized. However, their rates of formation and the tendency to give a 1:1 adduct $[LCu(O_2)]^+$ or a 2:1 adduct $[\{LCu\}_2(O_2)]^{2+}$ depends on the identity of the tripodal ligand involved.

(69) Sorrell, T. N.; Jameson, D. L. *Inorg. Chem.* **1982**, *21*, 1014–1019.

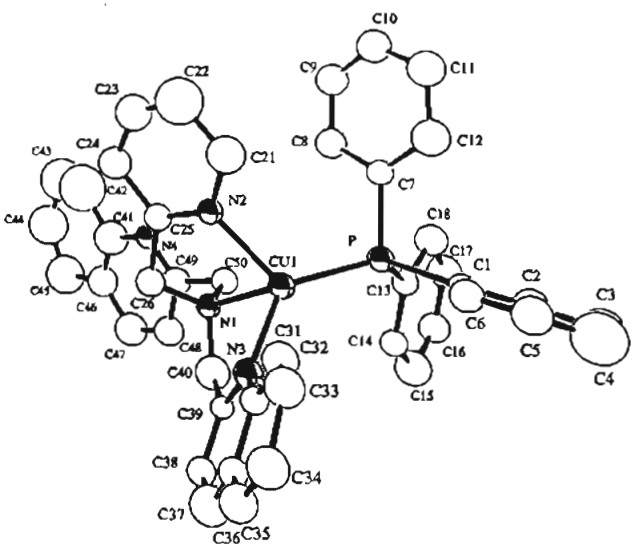

Figure 2. ORTEP diagram (30% ellipsoids) of the cationic portion of $[(BQPA)Cu(PPh_3)]^+$ (**3d**) showing the atom-labeling scheme.

Table 5. Cyclic Voltammetry Data for Cu(I) Complexes in DMF

complex	$E_{1/2}$, V	ΔE_p, mV	i_{pa}/i_{pc}
$[(TMPA)Cu(CH_3CN)]^+$ (**1a**)	–0.61	78	0.80
$[(TMPA')Cu(CH_3CN)]^+$ (**1a'**)	–0.56	88	0.85
$[(BPQA)Cu]^+$ (**2a**)	–0.53	85	0.96
$[(BQPA)Cu]^+$ (**3a**)	–0.41	95	0.96
$[(TMQA)Cu]^+$ (**4a**)	–0.24	108	1.02

Low-Temperature O_2 Reactivity of Cu(I) Complexes 1a–3a. The X-ray structurally characterized Cu_2O_2 species, the *trans*-μ-1,2-peroxo complex $[\{(TMPA)Cu\}_2(O_2)]^{2+}$ (**1c**), is formed from the reaction of $[(TMPA)Cu(CH_3CN)]^+$ (**1a**) with O_2 at –80 °C in EtCN or CH_2Cl_2 (Cu:O_2 = 2:1, manometry) with $K_{eq} = 4.3 \times 10^{11}$ M^{-2} at –90 °C.[7] The spectroscopic, physical, and reactivity properties of **1c** have been described in detail.[9,13,15]

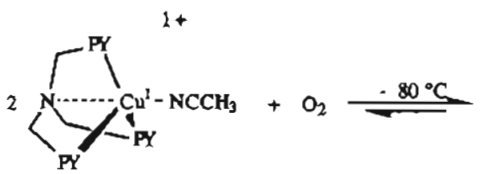

$[(TMPA)Cu(RCN)]^+$ (**1a**)

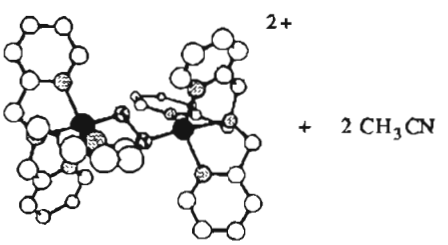

$[\{(TMPA)Cu\}_2(O_2)]^{2+}$ (**1c**)

Stopped-flow kinetic studies indicate that $[(TMPA)Cu(CH_3CN)]^+$ (**1a**) initially reacts to given an intermediate CuO_2 1:1 adduct $[(TMPA)Cu(O_2)]^+$ (**1b**). Complete data analyses deduced the detailed low-temperature oxygenation reaction mechanism given in Scheme 2, which was also shown to apply to dioxygen reactions with $[(BPQA)Cu]^+$ (**2a**) and $[(BQPA)Cu]^+$ (**3a**).[6,7] However, the behaviors of **1a**–**3a** differ considerably in detail, as also indicated by the chemical/spectroscopic studies described below. In particular, these reveal the properties of the novel 1:1 CuO_2 adduct $[(BQPA)Cu(O_2)]^+$ (**3b**), which is the thermodynamic product of the reaction of O_2 with **3a** and which can be readily studied in solution at –80 °C.

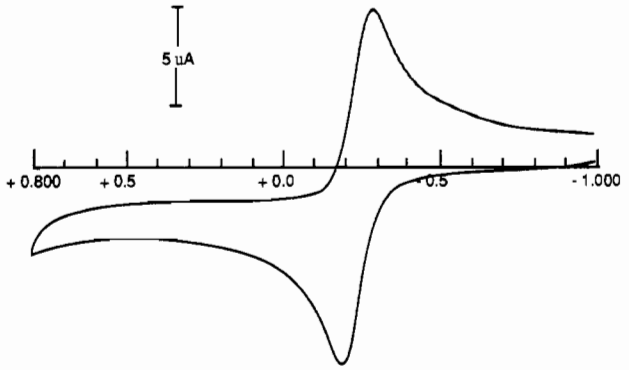

Figure 3. Cyclic voltammogram of $[(TMQA)Cu]^+$ (**4a**) in DMF at room temperature.

Scheme 2

$$[LCu(RCN)]^+ \quad (\mathbf{1a\text{-}3a}) \quad + \quad O_2 \quad \underset{k_{-1}}{\overset{k_1}{\rightleftharpoons}} \quad [LCuO_2]^+ \quad (\mathbf{1b\text{-}3b}) \quad + \quad RCN \qquad (1)$$

$$[LCuO_2]^+ \quad (\mathbf{1b\text{-}3b}) \quad + \quad [LCu(RCN)]^+ \quad (\mathbf{1a\text{-}3a}) \quad \underset{k_{-2}}{\overset{k_2}{\rightleftharpoons}} \quad [\{LCu\}_2O_2]^{2+} \quad (\mathbf{1c\text{-}3c}) \quad + \quad RCN \qquad (2)$$

Table 6. UV–Vis Spectral Data for Cu(I) Complexes and Their Dioxygen Complexes in EtCN

		UV–vis bands for dioxygen complexes (–80 °C)	
Cu^I complex	Cu^I band λ_{max}, nm (ϵ, M^{-1} cm^{-1})	$(LCu)\text{-}O_2$ λ_{max}, nm (ϵ, M^{-1} cm^{-1}) **1b, 3b**	$(LCu)_2\text{-}O_2$ λ_{max}, nm (ϵ, M^{-1} cm^{-1}) **1c–3c**
$[(TMPA)Cu(RCN)]^+$ (**1a**)	343 (5630)	410 (4000) 747 (1000)	525 (11 500) 590 (7600) 440 (4000) 1035 (160)
$[(BPQA)Cu]^+$ (**2a**)	303 (5700)		535 (10 500) 600 (7600) 440 (2000)
$[(BQPA)Cu]^+$ (**3a**)	303 (9300)	378 (8200)	545 (apparent 390)

Low-Temperature Reaction of O_2 with $[(BPQA)Cu]^+$ (2a). The copper(I) complexes used for low-temperature UV–vis and all reactivity studies reported below are the PF_6^- complexes of **2a** and **3a**, unless otherwise stated.

Manometric measurements for **2a** at –80 °C were carried out in order to confirm the stoichiometry of the reaction with O_2. The results show that the absorption of dioxygen by **2a** is in the ratio of $Cu:O_2 = 2.07(\pm 0.10):1$; thus, the product is a Cu_2O_2 2:1 adduct, formulated as $[\{(BPQA)Cu\}_2(O_2)]^{2+}$ (**2c**).

At –80 °C, in propionitrile solvent, a yellow Cu(I) complex $[(BPQA)Cu]^+$ (**2a**) exhibits a UV spectrum with increasing absorption toward higher energy with a shoulder ca. 325 nm. Upon addition of O_2 at –80 °C, the solution becomes intensely purple with UV–vis features at λ_{max} 535 (ϵ = 10 500 M^{-1} cm^{-1}), ca. 440 (sh, ϵ = 2000 M^{-1} cm^{-1}), and ca. 600 nm (sh, ϵ = 7600 M^{-1} cm^{-1}) (Table 6). The spectrum of $[\{(BPQA)Cu\}_2(O_2)]^{2+}$ (**2c**) is shown in Figure 4; it is almost identical to that of $[\{(TMPA)Cu\}_2(O_2)]^{2+}$ (**1c**). The close similarity of the spectrum and O_2-binding stoichiometry leads us to suggest that **2c** possesses a similar structure, i.e., a *trans*-(μ-1,2-peroxo)dicopper(II) unit, with analogous spectroscopic assignments (vide supra).

Reaction of PPh_3 and H^+ with $[\{(BPQA)Cu\}_2(O_2)]^{2+}$ (2c). PPh_3 is known as a good ligand for Cu(I) complexes, and it is often used in the characterization of the reactivity of Cu_nO_2 or other metal–dioxygen complexes.[15] Complex **2c** reacts with 2 equiv of PPh_3 at low temperature to form a Cu(I)–PPh_3 complex with concomitant liberation of O_2; the latter was qualitatively detected by letting the solution gradually warm to –65 °C and passing the gas evolved through an alkaline pyrogallol test solution, which turns from colorless to dark brown on exposure to dioxygen.[15] The reaction with PPh_3 did not occur as rapidly as that for $[\{(TMPA)Cu\}_2(O_2)]^{2+}$, where O_2 was liberated even at –80 °C after adding PPh_3 to solution of **1c**.[9] We suppose that the slower reaction of copper–dioxygen complex **2c** with PPh_3 may be due to steric hindrance imposed by the bulky quinolyl group of BPQA. As the reaction with PPh_3 proceeded, the intense purple color of **2c** diminished and a light green solution formed. A light green solid was obtained by precipitation with diethyl ether, and after recrystallization from acetonitrile/ether, a pale yellow complex, $[(BPQA)Cu(PPh_3)](PF_6)\cdot{}^1/_4Et_2O$ (**2d**-$(PF_6)\cdot{}^1/_4Et_2O$) could be obtained in 62% yield. This was characterized by ^1H NMR spectroscopy, and its properties were found to match those of the similar complex generated by the direct reaction of $[(BPQA)Cu(PPh_3)]^+$ (**1a**) with PPh_3 (vide supra). The green color observed is presumed to be due to small amount of oxidized impurities present before the fractional crystallization.

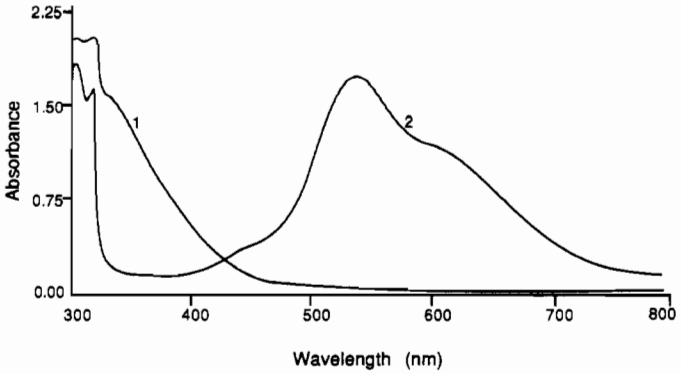

Figure 4. Low-temperature UV–vis spectra of $[(BPQA)Cu]^+$ (**2a**, spectrum 1) and $[\{(BPQA)Cu\}_2(O_2)]^{2+}$ (**2c**, spectrum 2).

Reactions of copper–dioxygen complexes with protonic acids have also been found to be useful in their characterization.[15] Typically, the copper–dioxygen complex $[\{(BPQA)Cu\}_2(O_2)]^{2+}$ (**2c**) was generated *in situ* by bubbling dry dioxygen gas through a Cu(I)–propionitrile solution (Cu(I) 0.3–0.5 mmol). Then, a 5-fold excess of $HBF_4\cdot Et_2O$ (1.5–2.5 mmol) was added to this solution. After workup (Experimental Section), hydrogen peroxide liberated was determined iodometrically. The high yield of H_2O_2 obtained (94%) indicates that the O–O bond is unbroken and the peroxo ligand is basic in nature.[15] The results compare well with those observed for addition of acid to $[\{Cu(TMPA)\}_2(O_2)]^{2+}$ (**1c**).[15]

Low-Temperature Reaction of O_2 with $[(BQPA)Cu]^+$ (3a): 1:1 CuO_2 Adduct Formation. Manometric measurements were also carried out for the O_2 reaction with **3a**. At –80 °C, the ratio $Cu:O_2 = 1.01(\pm 0.05):1$, suggesting a final 1:1 adduct $[(BQPA)Cu(O_2)]^+$ (**3b**) was formed. This strands in marked contrast to the stoichiometry of reaction observed for either **1a** or **2a** with O_2. Thus **3b** is a 1:1 adduct, presumably better described as a superoxo (i.e., O_2^-) copper(II) complex.

When a yellow Cu(I) solution (10^{-3}–10^{-4} M) of $[(BQPA)Cu]^+$ (**3a**) was oxygenated at –80 °C in propionitrile, an intensely purple solution initially formed; this was due to the presence of the 2:1 Cu_2O_2 adduct, $[\{(BQPA)Cu\}_2(O_2)]^{2+}$ (**3c**); vide infra. However, this color quickly disappeared and the solution transformed to a brown color, ascribed to the 1:1 CuO_2 adduct $(BQPA)Cu(O_2)]^+$ (**3b**). The complete formation of the brown species **3b** occurred after 5–8 min (at –80 °C), on the basis of attainment of the maximal absorption at 378 nm, and the resulting

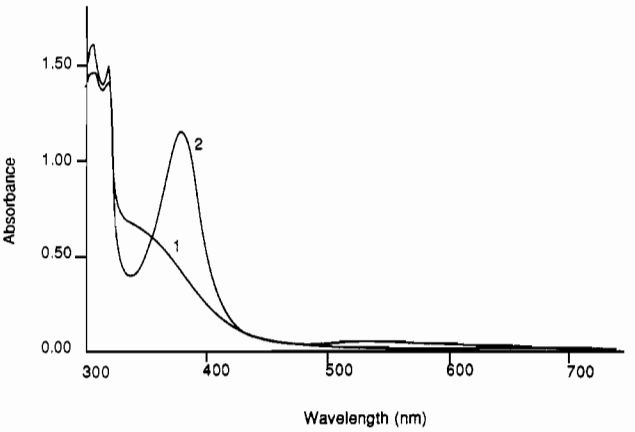

Figure 5. Low temperature UV–vis spectra of $[(BQPA)Cu]^+$ (**3a**, spectrum 1) and $[(BQPA)Cu(O_2)]^+$ (**3b**, spectrum 2).

species is stable at this temperature with PF_6^- as anion, while it is somewhat less stable using the ClO_4^- salt. The UV–vis spectra of **3a** and dioxygen adduct **3b** are shown in Figure 5, while absorption maxima and molar extinction coefficients are listed together with those determined for $[\{(BPQA)Cu\}_2(O_2)]^{2+}$ (**3c**) in Table 6.

The UV–vis absorption characteristics of $[(BQPA)Cu(O_2)]^+$ (**3b**) and $[\{(BQPA)Cu\}_2(O_2)]^{2+}$ (**3c**) have been separately confirmed in the low-temperature stopped-flow kinetic study (utilizing rapid-scanning diode-array UV–vis spectroscopy).[7] The λ_{max} of 378 nm (ϵ = 8200 M^{-1} cm^{-1}) for $[(BQPA)Cu(O_2)]^+$ (**3b**) presumably arises from a LMCT transition, formally O_2^--to-Cu(II). However no detailed spectroscopic studies have been carried out to confirm this, in large part because **3b** is one the very few reasonably well-characterized complexes with such an $LCuO_2$ formulation. The weaker absorption at 545 nm (Figure 5 and Table 6), with apparent ϵ = 390 M^{-1} cm^{-1}, is from neither a d–d absorption nor a charge-transfer transition. Rather, the kinetics study[7] shows that is due to the presence of a small amount of the dinuclear peroxodicopper(II) species $[\{(BQPA)Cu\}_2(O_2)]^{2+}$ (**3c**) which remains in a steady-state concentration during the oxygenation of $[(BQPA)Cu]^+$ (**3a**). The short lifetime (stopped-flow time scale) of **3c** precludes its practical observation in our "bench-top" oxygenation (by bubbling) and UV–vis experiments although, as indicated above, a purple "flash" can be initially observed. The kinetics study unambiguously shows that the oxygenation of **3a** follows that outlined in Scheme 2. In contrast to the oxygenation of $[(TMPA)Cu(CH_3CN)]^+$ (**1a**), the intermediate $[(BQPA)Cu(O_2)]^+$ (**3b**) does not build up in the initial stages of the reaction, but instead it rapidly converts to the 2:1 adduct $[\{(BQPA)Cu\}_2(O_2)]^{2+}$ (**3c**). However, the latter is not *thermodynamically* stable, and its reverts to **3b**.

The superoxocopper(II) description of the 1:1 CuO_2 adduct $[(BQPA)Cu(O_2)]^+$ (**3b**) would suggest it is a diamagnetic complex, since spin-pairing of a directly bonded O_2^- ligand with an Cu(II) ion, each with one unpaired electron, would lead to strong coupling. Consistent with this is the observed EPR silence of solutions of **3b**. Unfortunately, we were unable to obtain any –80 °C ^1H NMR spectra of **3b**, because of extreme difficulties in handling the thermally sensitive solution for insertion into an NMR spectrometer.

Reaction of PPh_3 and H^+ with $[(BQPA)Cu(O_2)]^+$ (3b). Complex **3b** reacted with 2 equiv of PPh_3 at low temperature to form a Cu(I)–PPh_3 complex with concomitant liberation of O_2; the latter was qualitatively detected by using a pyrogallol test solution when the **3b** with PPh_3 solution was gradually warmed to –45 °C. The still qualitatively slower reaction of complex **3b** with PPh_3 compared to those of **1c** and **2c** can be ascribed to the greater steric hindrance imposed by the two bulky quinolyl groups of BQPA. As the reaction proceeded, the intense brown color

Scheme 3

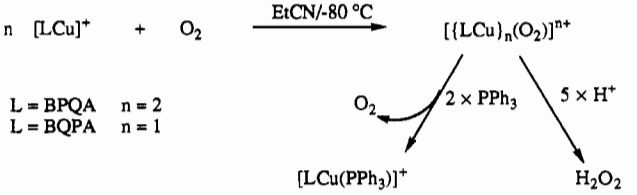

of copper–dioxygen complex **3b** diminished and a light green solution formed. A solid was obtained by precipitation with diethyl ether, and after recrystallization from acetonitrile/diethyl ether, a pale yellow complex of $[(BQPA)Cu(PPh_3)]PF_6 \cdot {}^1/_4Et_2O$ (**3d-(PF_6)·$^1/_4Et_2O$**) was obtained (58% yield). This was characterized by ^1H NMR spectroscopy and has spectroscopic properties identical to those of $[(BQPA)Cu(PPh_3)]ClO_4$ (**3d–ClO_4**), which was generated by the direct reaction of $[(BQPA)Cu]ClO_4$ (**3a–ClO_4**) with PPh_3.

Protonation of a –80 °C solution of $[(BQPA)Cu(O_2)]^+$ (**3b**) by addition of excess of $HBF_4 \cdot Et_2O$ gave an 89% yield of H_2O_2. The calculated yield presumes the reaction $2CuO_2 + 2H^+ \rightarrow 2HO_2 \rightarrow H_2O_2$, which is the same overall reaction stoichiometry expected for the reaction of a 2:1 Cu_2–O_2 adduct, e.g., that observed previously for $[\{(TMPA)Cu\}_2(O_2)]^{2+}$ (**1c**)[9] or here for $[\{(BPQA)Cu\}_2(O_2)]^{2+}$ (**2c**). Thus, the results indicate that the O–O bond in **3b** is unbroken and that the superoxo ligand is basic in nature.[15]

Thus, reactions of H^+ and PPh_3, with either 1:1 (Cu–O_2) or 2:1 (Cu_2–O_2) complexes **2c** or $[(BQPA)Cu(O_2)]^+$ (**3b**) can be summarized as indicated in Scheme 3.

TMPA-Transfer Reaction. To provide further evidence and verification that the 378-nm band corresponded to a copper–dioxygen complex $[\{(BQPA)Cu\}(O_2)]^+$ (**3b**), this was reacted with a solution of the TMPA ligand. From the kinetics/thermodynamics investigation,[7] $[\{Cu(TMPA)\}_2(O_2)]^{2+}$ (**1c**) has been shown to have a considerably greater stability (i.e. $K_{formation}$) than either **3b** or **3c**; given the reversible nature of the reactions, we expected that **3b** might be converted to **1c**. This is indeed the case. When a TMPA solution at –80 °C was added to the brown solution of **3b** to which a vacuum had been applied in order to exclude any excess free dioxygen, the color instantly changed to purple. The spectrum of the purple species was exactly the same as that of the strongly absorbing $[\{Cu(TMPA)\}_2(O_2)]^{2+}$ (**1c**) (Table 6). A conversion of **3b** to **1c** to the extent of a 45% yield occurred, on the basis of the known molar extinction coefficient of **1c**. The relatively low percentage conversion in this reaction is probably due to the still substantial binding of the copper ion to the BQPA chelating ligand; the TMPA-transfer reaction would require that the copper ion switch from a BQPA to a TMPA ligation. A TMPA-transfer reaction has been more successfully (>75% conversion) applied in the case where the initial $Cu_2O_2^{2+}$ complex possesses the unidentate 1,2-dimethylimidazole (L) ligand, i.e., $[L_6Cu_2(O_2)]^{2+} + 2TMPA \rightarrow [\{Cu(TMPA)\}_2(O_2)]^{2+}$ (**1c**) + 6L.[70]

$$2[(BQPA)Cu(O_2)]^+ + 2TMPA \rightleftharpoons [\{(TMPA)Cu\}_2O_2]^{2+} + 2BQPA + O_2$$

Reversible O_2-Binding of $[(BQPA)Cu]^+$ (3a). "Vacuum Cycling". "Metal complexes that bind dioxygen reversibly are defined as compounds that, upon interaction with O_2, form discrete $M_n(O_2)$ species, with the O–O bond unbroken and for which the O_2 can be liberated by varying the external conditions."[71,72]

(70) Sanyal, I.; Strange, R. W.; Blackburn, N. J.; Karlin, K. D. *J. Am. Chem. Soc.* **1991**, *113*, 4692–4693.
(71) Niederhoffer, E. C.; Timmons, J. H.; Martell, A. E. *Chem. Rev.* **1984**, *84*, 137–203.
(72) Karlin, K. D.; Gultneh, Y. *J. Chem. Educ.* **1985**, *62*, 983–990.

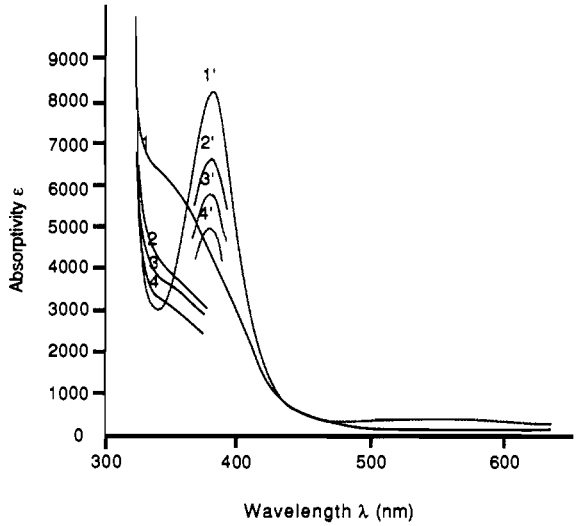

Figure 6. UV–vis spectra demonstrating the reversible O_2 binding behavior of $[(BQPA)Cu]^+$ (**3a**) (spectrum 1, solid line) in EtCN. Reaction of **3a** ($\sim 10^{-4}$ M) with O_2 at −80 °C generates the dioxygen adduct $[\{(BQPA)Cu\}(O_2)]^+$ (**3b**) (λ_{max} = 380 nm, spectrum 1′, shaded line). Removal of O_2 by brief heating to 100 °C along with vacuum/argon-purging regenerates **3a** (spectrum 2), and this process can be repeated several times, as shown.

Experiments illustrating repetitive cycling between $[(BQPA)Cu]^+$ (**3a**) and $[(BQPA)Cu(O_2)]^+$ (**3b**) are shown in Figure 6. The reversible dioxygen binding to $[(BQPA)Cu]^+$ (**3a**) is indicated by the ability to oxygenate this complex and deoxygenate $[(BQPA)Cu(O_2)]^+$ (**3b**), the latter by placing the solution under a static vacuum, followed by briefly (<5 s) immersing the solution into a boiling water bath; the solution immediately bleaches to give **3a** (Figure 6). The efficiency of the cycling experiments can be seen by the loss in the absorbance of the 378-nm band, 15%–18% per cycle, due to complex decomposition as a consequence of the heat treatment. Oxygenation of **3a** or warming of solutions of **3b** to room temperature results in the complex loss of the 378-nm absorption.

Possible Structure of the 1:1 Dioxygen Adduct (3b). As mentioned in the Introduction, 1:1 Cu(I)–O_2 adducts are of interest since they must represent primary interactions occurring in many copper protein systems. Further reaction and/or protonation of such species, e.g., giving a hydroperoxo Cu^{II}–OOH moiety, is directly relevant to monooxygenation chemistry, such as that occurring in dopamine β-hydroxylase.[39] Copper–dioxygen 1:1 complexes have long been proposed as intermediates present in Cu(I) autoxidation processes[73] and in the reaction of Cu(II) with superoxide in aqueous media.[74] As mimics for superoxide dismutase (SOD) and with the potential interests in therapeutic applications, reactions of superoxide with Cu(II) complexes have also being widely examined.[46,49,50,75-79]

However, structural, spectroscopic, and reactivity insights into CuO_2 complexes, i.e., superoxocopper(II) species, are greatly lacking. A number of reports of complexes of this type are noteworthy.[42,43,45] Valentine and co-workers[45] used UV–vis and EPR changes to indicate that a Cu(II)–O_2^- species can be synthetically generated *in situ* upon addition of 18-crown-6-solubilized KO_2 to solutions of the N_4 macrocyclic copper(II) complex Cu(tet b)$(ClO_4)_2$, (tet b = *rac*-5,7,7,12,14,14-hexamethyl-1,4,8,11-tetraazacyclotetradecane) in DMSO solvent. A new absorption at 672 nm was suggested to be of ligand field origin. By reaction of $[LCu^I(ethylene)]^+$ or $[LCu^I(CH_3CN)]^+$ (L = hydrotris(3,5-dimethyl-1-pyrazolyl)borate) with O_2, Thompson[42,43] isolated a stable solid compound formulated as $[LCu(O_2)]$ (L = hydrotris(3,5-dimethyl-1-pyrazolyl)borate; λ_{max} = 524 nm (ϵ = 600 M^{-1} cm^{-1})) with an assumed unsymmetrical end-on Cu(II)–O_2^-, coordinated structure. Kitajima has questioned the identity of this formulation, since dinuclear $\{Cu[HB(3,5\text{-}iPr_2pz)_3]\}_2(O_2)$ (*vide supra*) was synthesized under somewhat similar conditions.[3] Bailey et al.[49] noticed that addition of the superoxide anion to a tetraazaannulene–Cu(II) complex resulted in a doubling of observed vis spectral bands, and supporting electrochemical evidence was observed. Nishida and co-workers[47] observed marked increase absorbance at ~650 nm and in the 500–550-nm range, when superoxide was added to dimethyl sulfoxide solutions of a mononuclear Cu(II)–Schiff base complex. In our own laboratories, EPR and UV–vis spectrometries in addition to manometry (complex:O_2 = 1:1) were used in the solution characterization of a superoxide–dicopper(II) complex $[Cu_2(UN\text{–}O\text{–})(O_2)]^{2+}$. This is formed by the *reversible* reaction of dioxygen with the phenoxy-bridged mixed-valence dicopper complex $[Cu^ICu^{II}(UN\text{–}O\text{–})]^{2+}$.[44]

As mentioned above, no structural evidence is available for a superoxocopper(II) complex. Most often,[42,43] terminal end-on coordination is proposed, in a manner known to occur for many M–O_2 1:1 adducts such as oxy-hemoglobin or oxy-myoglobin and Schiff-base cobalt(III)–superoxo complexes.[25,26,28] However, η^2 side-on binding should be considered as a possibility for Cu–O_2 complexes, including $[(BQPA)Cu(O_2)]^+$ (**3b**). The superoxocobalt(III) complex $Tp'CO(O_2)$ (Tp′ = hydrotris(3-*tert*-butyl-5-methylpyrazolyl)borate) possesses such a binding configuration, as recently confirmed in an X-ray crystallographic study.[80]

Dioxygen complexes with side-on peroxo (formally) binding to both early and heavy transition metals are well-known, such as for Co(I), Ir(I), Pt(0), and Pd(0).[25] Also, as mentioned earlier, Kitajima has described a bridged η^2:η^2 side-on peroxo dinuclear complex, $\{Cu[HB(3,5\text{-}iPr_2pz)_3]\}_2(O_2)$ (vide supra).[36]

It is interesting to compare the properties of the 1:1 copper–dioxygen adduct $[(BQPA)Cu(O_2)]^+$ (**3b**) with those of the 1:1 adduct observed in the $[(TMPA)Cu]^+$ (**1a**) oxygenation reaction, i.e., $[\{(TMPA)Cu\}(O_2)]^+$ (**1b**). The latter could only be observed spectrophotometrically at −90 to −75 °C by using a stopped-flow instrument, since the kinetically (and thermodynamically) stable product observed is the 2:1 adduct $[\{(TMPA)Cu\}_2(O_2)]^{2+}$ (**1c**). With the BQPA ligand, the 1:1 adduct **3b** is instead observed as the final stable species at −80 °C. We largely attribute this differing behavior to steric factors, i.e., the bulky ligand environment provided by the quinolyl donor groups in copper complexes containing BQPA. $[(BQPA)Cu(O_2)]^+$ (**3b**) would thus be far less accessible for attack by another copper(I) mononuclear complex $[(BQPA)Cu]^+$ (**3a**) in forming a 2:1 adduct $[\{(BQPA)Cu\}(O_2)]^{2+}$ (**3c**) (Scheme 2). The more positive redox potential (i.e. favoring Cu(I) compared to Cu(II)) of BQPA copper complexes (Table 5) also lessens the driving force for attack of **3b** by **3a** to form **3c**, i.e. in the reduction of a Cu(II)–O_2^- species to a peroxodicopper(II) complex. However, this may not be the determining factor, as discussed further below. Here also, an important observation is that since we know that **3c** briefly forms during the oxygenation reaction of **3a**,[7] steric factors, e.g., bumping

(73) Zuberbühler, A. D. In *Metal Ions in Biological Systems*; Sigel, H., Ed.; Marcel Dekker: New York, 1976; Vol. 5, pp 325–368.
(74) Meisel, D.; Levanon, H.; Czapski, G. *J. Phys. Chem.* **1974**, *78*, 779–782.
(75) Czapski, G.; Goldstein, S.; Meyerstein, D. *Free Radical Res. Commun.* **1988**, *4*, 231–236.
(76) Goldstein, S.; Czapski, G. *Free Radical Res. Commun.* **1991**, *12–13*, 205–210.
(77) Strothkamp, K. G.; Lippard, S. J. *Acc. Chem. Res.* **1982**, *15*, 318–326.
(78) Roberts, J. L., Jr.; Sawyer, D. T. *Isr. J. Chem.* **1983**, *23*, 430–438.
(79) Tait, A. M.; Hoffman, M. Z.; Hayon, E. *Inorg. Chem.* **1976**, *15*, 934.
(80) Egan, J. W., Jr.; Haggerty, B. S.; Rheingold, A. L.; Sendlinger, S. C.; Theopold, K. H. *J. Am. Chem. Soc.* **1990**, *112*, 2445–2446.

of quinolyl groups from ligands on adjacent Cu ions, must be responsible for the stabilization of the 1:1 adduct $[(BQPA)Cu(O_2)]^+$ (**3b**). Steric effects leading to the formation of a 1:1 iron–dioxygen adduct by suppressing the formation of the (μ-peroxo)diiron complex have been observed in iron porphyrin model systems as well, such as the classic case of a picket fence porphyrin.[81-83] In such protected porphyrin systems, the formation of $LFe^{III}–O_2–Fe^{III}L$ from $LFe^{II}–O_2 + LFe^{II}$ is prevented due to the bulky porphyrin side groups.

It is also noteworthy that the thermodynamic stabilities of the 1:1 Cu–O_2 adducts $[\{(TMPA)Cu\}(O_2)]^+$ (**1b**) and $[(BQPA)Cu(O_2)]^+$ (**3b**) are essentially identical, in spite of the difference in Cu(II)/Cu(I) redox potential of the two Cu(I) precursor complexes (~0.19 V, Table 5). If electronic effects were significant, a favoring of O_2-binding stability in $[\{(TMPA)Cu\}(O_2)]^+$ (**1b**) would be suggested. The equilibrium constants at 183 K for formation of **1b** and **3b** are $(1.9 \pm 0.1) \times 10^3$ and $(2.9 \pm 0.3) \times 10^3\ M^{-1}$, respectively; standard enthalpies and entropies of formation are also very comparable.[7] *Steric and not electronic factors seem to predominate.* From a large body of data concerning many kinds of cobalt chelate Cu:O_2 = 1:1 dioxygen carriers, electronic factors such as Co(II)/Co(III) redox potentials correlate in many cases, but exceptions do occur.[71] In the present system, differences in TMPA and BQPA would suggest that structural variations in the LCu–O_2 moiety are likely, thus obviating the occurrence of a linear free energy relationship such as one between metal–complex redox potential and K_{eq} for O_2-binding. Supporting a possible structural difference in Cu–O_2 adducts **1b** and **3b** are their markedly different UV–vis characteristics; for **1b** maxima are observed at 410 nm (ϵ = 4000 M^{-1} cm^{-1}) and 747 nm (ϵ = 1000 M^{-1} cm^{-1}), while λ_{max} for **3b** is 378 nm (ϵ = 8200 M^{-1} cm^{-1}) (Table 6). A complete spectral analysis of these presumed charge-transfer transitions is required. Local variations in coordination environment are most likely due to subtle but important changes in medium (e.g., dielectric) and sterically enforced changes in ligand-binding geometry, all caused by differences in the pyridyl versus quinolyl rings.

Reactivity of $[(TMQA)Cu]ClO_4$ and $[(TMQA)Cu]PF_6$ (4a). Both of these complexes are unreactive toward dioxygen in the solid state. In acetonitrile solution, **4a**-ClO_4 is very stable in an O_2 atmosphere, while **4a**-PF_6 undergoes very slow (e.g., in days) decomposition. The stability of $[(TMQA)Cu]^+$ (**4a**) in principle could be explained by factors relating to both its redox potential and its bulky structure. The very positive $E_{1/2}$ value (Table 5) would suggest that this complex is difficult to oxidize (i.e., by O_2) and favors the lower oxidation state Cu(I). Thus, initial binding of O_2 to form a 1:1 adduct would be unfavorable, since the one-electron reduction of O_2 to the superoxide anion is also unfavorable.[26,71,84] Thus, the equilibrium in eq 1 (Scheme 2) may lie far to the left for TMQA. Furthermore, subsequent reaction of a putative 1:1 adduct $[(TMQA)Cu(O_2)]^+$ with Cu(I) complex **4a** would also not be favored, since the driving force for Cu(I) → Cu(II) is low.

However, without proof that electronic considerations absolutely prevent Cu(I)/O_2 electron-transfer reactions of $[(TMQA)Cu]^+$ (**4a**), the lack of reactivity could still be explained as being due to steric effects. The crystal structure of $[(TMQA)Cu]^+$ (**4a**) reveals the ligation to be pseudotetrahedral, such that the Cu(I) ion lies on one side of the plane of the quinolyl N atoms, toward the N1 alkylamine N donor (Figure 1). Thus it is quite far away and protected by the quinolyl donors from ligation by an additional exogenous ligand donor such as O_2. We do know, however, that coordination of additional ligands is possible: (i) Earlier in the discussion (vide supra), we suggested that CH_3CN solvent can bind to Cu(I), perhaps by weakening of the Cu(I)–alkylamino N atom coordination, as in $[(TMPA')Cu(RCN)]^+$ (**1a'**) [with Cu–N ~ 2.439 (8) Å] or by release and dangling of one quinolyl donor, as in $[(BQPA)Cu(PPh_3)]^+$ (**3d**). (ii) In a separate study, the Cu(II) complex $[(TMQA)Cu^{II}Cl]^+$ has been isolated and characterized by X-ray crystallography.[85] Thus, a small ligand like O_2 might bind to the copper ion in a TMQA ligand environment, but perhaps a *bent* end-on or an η^2 side-on Cu–O_2 structure is precluded by steric interactions of the proximate quinolyl groups in a complex with TMQA; there is, after all, one pyridyl donor in $[(BQPA)Cu(O_2)]^+$ (**3b**). In any case, further reaction of a putative species $[(TMQA)Cu(O_2)]^+$ (**4b**) with a second molecule of **4a** is not likely allowed sterically. The net result is the observed lack of reactivity of O_2 toward **4a**. These ideas are in accordance with a large body of kinetic data, primarily from Zuberbühler and co-workers, indicating that it is the reaction of $[LCuO_2]^+$ with $[LCu]^+$ that drives the chemistry toward Cu_2O_2 formation,[73] since the one-electron O_2 to O_2^- reduction is thermodynamically unfavorable.[25,71,84]

Conclusion

By synthesizing mononuclear copper complexes with tripodal tetradentate ligands containing different numbers of quinolyl groups, it is possible to obtain $Cu_n–O_2$ complexes of varying stoichiometry, n = 1 and n = 2. For the parent $[(TMPA)Cu(RCN)]^+$ (**1a**) complex at low temperature, both 1:1 and 2:1 copper dioxygen adducts were observed in a stopped-flow kinetics study, and the dicopper(II) peroxo complex $[\{(TMPA)Cu\}_2(O_2)]^{2+}$ (**1c**) with *trans*-μ-1,2-peroxo-bridged binding is the final isolable thermodynamically stable species. When one pyridyl group is replaced by one quinolyl donor, only the final stable 2:1 adduct $[\{(BPQA)Cu\}_2O_2]^{2+}$ (**2c**) is observed. This occurs because the disappearance rate for the 1:1 species is greater than its formation rate in the observed experimental temperature range.[7] Thus, no 1:1 adduct accumulates, at least not at temperatures as low as –90 °C. For the BQPA ligand, where two pyridyl groups are replaced by quinolyl donors, again both 1:1 and 2:1 adducts have been detected. However, the stability of the 2:1 adduct is rather small, largely due to steric hindrance effects. An overshooting is seen in kinetics studies,[7] i.e., a rapid formation of a 2:1 adduct which then quickly reverts to a 1:1 adduct $[\{(BQPA)Cu\}(O_2)]^+$ (**3b**) and $[(BQPA)Cu]^+$ (**3a**). Eventually, nearly all the **3a** present transforms to the final stable 1:1 adduct which we observe and can study on the slower time scale of low-temperature bench-top chemistry, as detailed in this report. Finally, for TMQA with three quinolyl donors, no Cu(I)/O_2 reaction whatsoever is observed. The observed copper(I)/O_2 chemistry with complexes of TMPA, BQPA, and TMQA ligands leads to the argument that *steric effects may predominate in determining O_2-reaction chemistry*. This conclusion, along with the ability to manipulate and study both 1:1 and 2:1 copper–dioxygen adducts, is perhaps the most important outcome of the present study.

It is encouraging to synthetic chemists that small changes in the tripodal ligand employed allow for study of a variety of species, since such changes cause dramatic differences in the relative stabilities of various types of copper–dioxygen complexes, i.e. 1:1 or 2:1 Cu/O_2 adducts. A recent report[86] indicates that systematically varied 6-methyl substitution of pyridyl rings on TMPA type ligands (L'') also dramatically affects the thermal stability or spectroscopy of resulting $L''_2Cu_2–O_2$ adducts; however, no evidence for Cu:O_2 = 1:1 adducts was obtained. It seems quite

(81) Collman, J. P., Gagne, R. R.; Reed, C. A.; Robinson, W. T.; Rodley, G. A. *Proc. Natl. Acad. Sci. U.S.A.* **1974**, *71*, 1326.
(82) Collman, J. P., Gagne, R. R.; Reed, C. A.; Halbert, T. R.; Lang, G.; Robinson, W. T. *J. Am. Chem. Soc.* **1975**, *97*, 1427–1439.
(83) Collman, J. P.; Halpert, T. R.; Suslick, K. S. In *Metal Ion Activation of Dioxygen: Metal Ions in Biology*; Spiro, T. G., Ed.; Wiley-Interscience: New York, 1980; Vol. 2, pp 1–72.
(84) Jones, R. D.; Summerville, D. A.; Basolo, F. *Chem. Rev.* **1979**, *2*, 139–179.
(85) Wei, N.; Karlin, K. D. Unpublished results.
(86) Uozumi, K.; Hayashi, Y.; Suzuki, M.; Uehara, A. *Chem. Lett.* **1993**, *6*, 963–966.

possible to control the observed chemistry and to therefore impart various design features. Isolation of stable Cu:O_2 = 1:1 adducts and their derivatives, accompanied by spectroscopic and reactivity studies, is a subject of current concern.

Experimental Section

Materials and Methods. Reagents and solvents used were of commercially available reagent quality unless otherwise stated. Dioxygen gas was dried over a short column of supported P_4O_{10} (Aquasorb, Mallinkrodt). Propionitrile was first distilled over P_4O_{10}, then refluxed, and distilled from CaH_2 under argon. Anhydrous diethyl ether was used by passing it through a 50-cm column of activated alumina or it was directly distilled from sodium/benzophenone under argon. All ligands were synthesized and characterized in the air, unless otherwise stated. Column chromatography was carried out on alumina, unless otherwise stated. Preparation and handling of air-sensitive materials were carried out under an argon atmosphere by using standard Schlenk techniques. Deoxygenation of solvents and solutions were effected by either repeated vacuum/purge cycles using argon or bubbling of argon (20 min) directly through the solution. Solid samples were stored and transferred, and samples for NMR and IR spectra were prepared in a Vacuum/Atmospheres drybox filled with argon. Elemental analyses were performed by Desert Analytics, Tucson, AZ.

Infrared spectra were recorded on neat samples or in Nujol mulls on a Mattson Galaxy 4030 FT-IR spectrometer. NMR spectra were measured in $CDCl_3$, CD_3CN, and CD_2Cl_2 on either a Varian (400 MHz) or a Bruker (300 MHz) spectrometer. All spectra were recorded in 5-mm-o.d. NMR tubes. Chemical shifts were reported as δ values downfield from an internal standard of Me_4Si. Electron paramagnetic resonance (EPR) spectra were obtained on frozen solutions at 77 K with 4-mm-o.d. quartz tubes in a Varian Model E-4 spectrometer operating at X-band frequency. The field was calibrated with a powder sample of diphenylpicrylhydrazyl (DPPH; g = 2.0037). The solvent used was propionitrile with the concentration of the copper complex at $\sim 10^{-3}$ M. The signal obtained was roughly integrated by comparing the intensity observed ($I = h_{1/2}(w_{1/2h})^2$) with that of known concentration of [(TEPA)-Cu(Cl)]PF_6[67] in DMF. The room-temperature electron absorption spectra were recorded on a Shimadzu UV-160 spectrometer using quartz cuvettes (1 cm). Low-temperature electron spectroscopic studies were carried out by using a Hewlett-Packard 8452A diode array spectrometer driven by a Compaq Desk pro 386S computer using software written by On-Line Instrument Systems, Inc. The spectrometer was equipped with a variable-temperature Dewar flask and a cuvette assembly as described elsewhere.[58,61] Gas chromatography was carried out on a Hewlett-Packard 5890 instrument fitted with a 30m HP-5 (cross-linked 5% phenyl methyl silicone) capillary column. Electron ionization mass spectra were obtained on a double-focusing Vacuum Generator 70-S (VG-70S) gas chromatography/mass spectrometer.

Synthesis of Ligands. 2-(Bromomethyl)quinoline.[87] To a 250-mL round-bottom flask was added 150 mL of benzene. In the following order were added *N*-bromosuccinimide (NBS) (42.0 g, 235 mmol), quinaldine (30.0 g, 210 mmol), and benzoyl peroxide (1.0 g, 4 mmol) with stirring. The solution was refluxed for 3.5 h under UV light. During this time, the insoluble NBS gradually dissolved and the solution became red. After the reaction was complete, the solution was allowed to cool to precipitate all succinimide until no yellow color formed when 5% HBr was added. The precipitate was filtered off, and the resulting red solution was concentrated *in vacuo* to give a reddish oil. This was washed in several portions with ~400 mL of 5% HBr solution to generate, upon stirring, a yellow aqueous solution and a brown sticky solid. The aqueous solution, which contained the 2-(bromomethyl)quinoline, was collected and neutralized with saturated Na_2CO_3 solution. As Na_2CO_3 solution was added, CO_2 gas was evolved and a yellow precipitate was formed. The precipitate was collected by filtration, and the filtrate was saved. The precipitate was recrystallized from hexane, and a white needlelike crystalline material was obtained. Additional crystals were obtained by extracting the filtrate with hexane (3 × 200 mL) and storing the extracts in a freezer overnight. The total amount of 2-(bromomethyl)quinoline produced was 41.3 g (45%). ^{1}H NMR ($CDCl_3$): δ 4.71 (s, 2 H, CH_2Br), 7.51–7.56 (t, 2 H), 7.69–7.81 (m, 2 H), 8.05–8.08 (d, 1 H), 8.13–8.16 (d, 1 H).

(87) Masaru, H. *Yakagaku Zasshi* **1951**, *71*, 256–259.

BPQA. In the following order, dipicolylamine[88] (Nepera) (2.00 g, 10 mmol), triethylamine (Et_3N) (2 mL, 14.2 mmol), and 2-(bromomethyl)-quinoline (2.23 g, 10 mmol) were added to 100 mL of tetrahydrofuran (THF). The solution mixture was stirred for 3 days at room temperature. With time, the solution became brown and a white precipitate formed. After filtering the solution, the filtrate was concentrated *in vacuo* to give a brown oil which was column chromatographed and eluted with ethyl acetate (R_f 0.5; alumina, ethyl acetate). The product fraction was collected, and the solution was concentrated *in vacuo* to give a light yellow solid which was recrystallized from diethyl ether to afford a white crystalline material (1.9 g, 56% yield). ^{1}H NMR ($CDCl_3$): δ 3.95 (s, 4 H, CH_2 of py), 4.05 (s, 2 H, CH_2 of quinolyl), 7.05 (t, 2 H), 7.4–7.84 (m, 8 H), 8.05 (m, 1 H), 8.16 (m, 1 H), 8.53 (d, 2 H, py 6-H). ^{13}C NMR ($CDCl_3$): δ 60.98 (CH_2 of py), 61.62 (CH_2 of quinolyl), 118.26, 122.03, 123.02, 123.95, 127.05, 128.65, 129.69, 130.26, 137.18, 137.32, 149.83, 160.35, 161.36.

BQPA. Diisopropylethylamine (iPr$_2$EtN) (6.3 g, 48.8 mmol) and 2-(bromomethyl)quinoline (5.43 g, 24.4 mmol) were added to 100 mL of THF. To this solution was added dropwise 2-(methylamino)pyridine (1.33 g, 12.2 mmol). The reaction mixture was stirred for 3 days at room temperature. With time, the solution changed from light yellow to orange and a white precipitate formed. After the solution was filtered, the filtrate was concentrated *in vacuo* to give a brown oil which was column chromatographed and eluted with ethyl acetate (R_f 0.6; alumina, ethyl acetate). The product fraction was collected, and the solution was concentrated *in vacuo* to give a light yellow solid, which was recrystallized from diethyl ether to afford a white crystalline material (3.1 g, 65% yield). ^{1}H NMR ($CDCl_3$): δ 3.97 (s, 2 H, CH_2 of py), 4.10 (s, 4 H, CH_2 of quinolyl), 7.12 (t, 1 H), 7.47–7.84 (m, 10 H), 8.02–8.08 (d, 2 H), 8.10–8.14 (d, 2 H), 8.52 (d, 1 H, py 6-H). ^{13}C NMR ($CDCl_3$), 60.03 (CH_2 of py), 60.60 (CH_2 of quinolyl), 120.60, 121.60, 122.75, 125.69, 126.86, 127.05, 128.60, 128.89, 135.88, 147.14, 148.65, 158.78, 159.60.

TMQA. To 80 mL of THF were added 2-(bromomethyl)quinoline (5 g, 22.5 mmol) and ammonium hydroxide (0.5 mL, 7.15 mmol) (density 14.8 g/mL). The clear solution was stirred. After $^1/_2$ h, the clear solution became cloudy. The solution mixture was allowed to stir for 1 week, resulting in a brown solution with a white precipitate. The mixture was filtered, and the precipitate was collected, washed with water and a minimal amount of methanol, and then dried under vacuum. After the filtrate was concentrated *in vacuo*, a brown oil with some solid was obtained. This material was dissolved in CH_2Cl_2, and the solution was washed with water. The organic layer was collected and dried over $MgSO_4$. The CH_2Cl_2 was removed under reduced pressure, resulting in a solid residue, which was washed with a minimal amount of methanol. From this, an additional amount of white precipitate formed and was collected. This precipitate was combined with the previous portion, affording an overall yield of 1.2 g of product (36%). Mass spectrum: m/z 440 (M^+), 441 ($(M + 1)^+$). ^{1}H NMR ($CDCl_3$): δ 4.13 (s, 6 H, CH_2), 7.50–7.52 (t, 3 H), 7.68–7.79 (m, 9 H), 8.05–8.08 (d, 3 H), 8.11–8.14 (d, 3 H).

Synthesis of Copper(I) Complexes. [(BPQA)Cu]PF_6 (2a-PF_6). Dioxygen-free CH_3CN (10 mL) was added to solids the BPQA (0.476 g, 1.40 mmol) and [Cu(CH_3CN)$_4$]PF_6 (0.5 g, 1.34 mmol) under argon. The solids quickly dissolved, and a yellow solution formed. The solution was allowed to stir for 15 min. Diethyl ether (100 mL) was added, resulting in the separation of an orange oil. After the clear supernatant was decanted, the oil was redissolved in 15 mL of CH_3CN. Diethyl ether (ca. 50 mL) was added to the yellow solution until a slight cloudiness developed. The solution was filtered under argon with a medium frit. An additional portion of dry ether was added to the clear yellow filtrate, resulting in the separation of an orange oil. The supernatant was decanted, and a vacuum was applied to the oil, giving a solid, which was washed with ether and dried *in vacuo*, resulting in 0.5 g of yellow powder (67% yield). Anal. Calcd for $CuC_{22}H_{20}N_4PF_6$: C, 48.17; H, 3.65; N, 10.21. Found: C, 48.85; H, 3.89; N, 10.35. ^{1}H NMR (CD_3CN): 4.05 (s, 4 H, CH_2 of py), 4.25 (s, 2 H, CH_2 of quinolyl), 7.32–8.59 (m, 14 H). IR (Nujol, cm^{-1}): 1599 (s, C=C), 840 (vs, PF_6^-).

[(BQPA)Cu]PF_6 (3a-PF_6). Dioxygen-free propionitrile (8 mL) was added to the solids BQPA (0.22 g, 0.56 mmol) and [Cu(CH_3CN)$_4$]PF_6 (0.2 g, 0.536 mmol) under argon. The solids quickly dissolved, and the solution became orange. The solution was stirred under argon for 15 min. Diethyl ether was added, resulting in the separation of an orange oil, which was redissolved in propionitrile; to this solution was added a small portion of dry ether until a slight cloudiness developed. The mixture

(88) Romary, J. K.; Zachairasen, D. R.; Barger, J. D.; Schiesser, H. *J. Chem. Soc. C* **1968**, 2884.

was filtered under argon with a medium frit. An additional portion of dry ether was added to the clear orange filtrate, resulting in the separation of an orange oil. The supernatants was decanted, and a vacuum was applied to the oil, giving a solid, which was washed with ether and dried under vacuum to give 0.28 g of yellow powder (88% yield). Anal. Calcd for $CuC_{26}H_{22}N_4PF_6$: C, 52.14; H, 3.70; N, 9.35. Found: C, 52.50; H, 3.84; N, 9.43. ^{1}H NMR (CD_3CN): 4.04 (s, 2 H, CH_2 of py), 4.24 (s, 4 H, CH_2 of quinolyl), 7.20–7.82 (m, 11 H), 8.18–8.20 (d, 2 H), 8.38–8.41 (d, 2 H), 8.53 (s, 1 H, py 6-H). ^{13}C NMR (CD_3CN): δ 61.5, 122.38, 124.41, 125.30, 127.96, 128.86, 129.35, 131.47, 137.96, 138.62, 149.80, 157.00, 158.98. IR (Nujol, cm^{-1}): 1599 (s, C=C), 841 (vs, PF_6^-).

[(BQPA)Cu]ClO_4 (3a-ClO_4). Dioxygen-free CH_3CN (10 mL) was added to the solids BQPA (1.5 g, 3.85 mmol) and $[Cu(CH_3CN)_4]ClO_4$ (1.14 g, 3.50 mmol) under argon. The solids quickly dissolved, and the solution became yellow. The yellow solution was stirred for 15 min under argon, whereupon diethyl ether was added to precipitate a yellow solid. This was redissolved in CH_3CN and precipitated with ether, giving a yellow microcrystalline material, which was washed with ether and dried *in vacuo* yielding 1.72 g (89%) of final product. *Caution! While we experienced no problems with this or other perchlorate salts, extreme care should be excercised in handling these potentially explosive complexes.* Anal. Calcd for $CuC_{26}H_{22}N_4ClO_4$: C, 56.42; H, 3.78; N, 10.13. Found: C, 56.65; H, 4.07; N, 10.43. ^{1}H NMR (CD_3CN): δ 4.04 (s, 2 H, CH_2 of py), 4.24 (s, 4 H, CH_2 of quinolyl), 7.20–7.82 (m, 11 H), 8.18–8.20 (d, 2 H), 8.38–8.41 (d, 2 H), 8.53 (s, 1 H, py 6-H). IR (Nujol, cm^{-1}): 1599 (s, C=C), 1090 (vs, ClO_4^-).

[(TMQA)Cu]PF_6 (4a-PF_6). Dioxygen-free CH_2Cl_2 (20 mL) was added to the solids TMQA (0.265 g, 0.59 mmol) and $[Cu(CH_3CN)_4]PF_6$ (0.200 g, 0.536 mmol) under argon. The solids gradually dissolved, and the solution became yellow. The yellow solution was allowed to stir for 15 min under argon, whereupon diethyl ether (80 mL) was used to precipitate a yellow solid. This was washed with ether and dried under vacuum, resulting in 0.26 g of yellow crystalline product (74%). Anal. Calcd for $CuC_{30}H_{24}N_4PF_6$: C, 55.52; H, 3.73; N, 8.63. Found: C, 55.64; H, 3.62; N, 8.78. ^{1}H NMR (CD_3CN): δ 4.46 (s, 6 H, CH_2 of quinolyl), 7.43 (d, 3 H), 7.57 (t, 3 H), 7.83 (t, 6 H), 8.22 (d, 3 H), 8.43 (d, 3 H). IR (Nujol, cm^{-1}): 1599 (s, C=C), 841 (vs, PF_6^-).

[(TMQA)Cu]ClO_4 (4a-ClO_4). Dioxygen-free CH_2Cl_2 (40 mL) was added to the solids TMQA (0.746 g, 1.69 mmol) and $[Cu(CH_3CN)_4]ClO_4$ (0.504 g, 1.54 mmol) under argon. The solids gradually dissolved, and the solution became yellow and was allowed to stir for 15 min. Diethyl ether (200 mL) was used precipitate a yellow crystalline solid. After filtration, the solid was washed with ether and dried under vacuum, resulting in 0.83 g of yellow crystalline material (89%). Anal. Calcd for $CuC_{30}H_{24}N_4ClO_4$: C, 59.70; H, 4.01; N, 9.28. Found: C, 59.16; H, 3.94; N, 9.07. ^{1}H NMR (CD_3CN): δ 4.46 (s, 6 H, CH_2 of quinolyl), 7.43 (d, 3 H), 7.57 (t, 3 H), 7.83 (t, 6 H), 8.22 (d, 3 H), 8.43 (d, 3 H). IR (Nujol, cm^{-1}): 1599 (s, C=C), 1090 (vs, ClO_4^-). Yellow X-ray quality crystalline **4a-(ClO_4)** was obtained by dissolving the Cu(I) complex in dioxygen-free CH_3CN and carefully layering ether on the solution. Crystals developed after 2–3 days.

[(BPQA)Cu(PPh_3)]PF_6 (2d-PF_6). Triphenylphosphine (0.143 g, 0.546 mmol) in 10 mL of dioxygen-free CH_3CN was added dropwise to [(BPQA)Cu]PF_6 (0.30 g, 0.546 mmol) under argon. The yellow solid quickly dissolved, and the solution was allowed to stir for 15 min under argon. Diethyl ether was added until a slight cloudiness developed; the mixture was filtered under argon using a medium frit. An additional portion of dry ether was added to the clear filtrate to precipitate an off-white solid, which was washed with ether and dried under vacuum, giving 0.28 g of product powder (63%). Anal. Calcd for $CuC_{40}H_{35}N_4P_2F_6$: C, 59.22; H, 4.35; N, 6.91. Found: C, 60.30; H, 4.37; N, 7.00. ^{1}H NMR (CD_3CN): δ 4.10 (s, 2 H, CH_2 of py), 4.31 (s, 4 H, CH_2 of quinolyl), 7.29, 7.49 (m, 22 H), 7.76 (2 H), 7.88 (b, 1 H), 8.20 (b, 1 H), 8.23 (d, 1 H), 8.45 (s, 2 H, py 6-H). IR (Nujol, cm^{-1}: 1599 (s, C=C), 841 (vs, PF_6^-).

[(BQPA)Cu(PPh_3)]ClO_4 (3d-ClO_4). Triphenylphosphine (0.146 g, 0.559 mmol) dissolved in 10 mL of dioxygen-free CH_3CN was added dropwise to solid [(BQPA)Cu]ClO_4 (0.302 g, 0.546 mmol), which quickly dissolved, and the solution became pale yellow. This was allowed to stir for 15 min under argon, whereupon diethyl ether was added until a slight cloudiness developed. The mixture was filtered under argon using a medium frit, and an additional portion of dry ether was added to the clear filtrate to precipitate an off-white solid. This was washed with ether and dried under vacuum, giving 0.32 g of powder product (72%). Anal. Calcd for $CuC_{44}H_{37}N_4ClO_4$: C, 64.79; H, 4.54; N, 6.87. Found: C, 64.67; H, 4.59; N, 6.79. ^{1}H NMR (CD_3CN): δ 4.04 (s, 2 H, CH_2 of py), 4.24 (s, 4 H, CH_2 of quinolyl), 7.20–7.82 (m, 26 H), 8.18–8.20 (d, 2 H), 8.38–8.41 (d, 2 H), 8.53 (s, 1 H, py 6-H). IR (Nujol, cm^{-1}): 1599 (s, C=C), 1084 (vs, ClO_4^-). X-ray-quality **3d-ClO_4** was obtained by dissolving ~0.1 g of the Cu(I) complex in ~10 mL of oxygen-free CH_3CN and then carefully layering ether upon this solution. Light yellow needle crystals developed after 2–3 days.

Gas (O_2) Uptake Manometry. O_2 absorption for complexes **2a** and **3a** at –80 °C was monitored at contsnt pressure by using a gas buret system as previously described.[61] When the O_2 absorption leveled off, the volume of O_2 absorbed by the copper(I) complex solution was recorded and the O_2 absorption by the pure propionitrile solvent was subtracted from it.

Methods To Generate $(Cu_n–O_2)^{n+}$ Species [{(BPQA)Cu}$_2$(O_2)]$^{2+}$ (2c) and [{(BQPA)Cu}(O_2)]$^+$ (3b). Copper complex **2a** was dissolved in dioxygen-free propionitrile solvent, and the solution was cooled to –80 to –90 °C by using a methanol/liquid nitrogen slush bath. Upon bubbling of dioxygen, the yellow Cu(I) solution immediately became intensely purple. The solution was completely oxygenated by bubbling dioxygen through it for 5 min. **3b** was generated by a similar procedure except that the yellow **3a** solution first became deep purple upon exposure to dioxygen and then completely became brown, forming **3b** after about 10 min.

EPR Measurements of [{(BQPA)Cu}(O_2)]$^+$ (3b). In a quartz EPR tube, a solution of **3a** in EtCN was bubbled with dioxygen (syringe needle); initially the solution turned purple, but after 5 min it became brown, characteristic of the 1:1 adduct. This solution was frozen (77 K) and inserted into the EPR instrument, and the spectrum was recorded.

Determination of O_2 Liberation from $(Cu_n–O_2)^{n+}$ Species. Qualitative Methods. These experiments were performed in a manner similar to that previously described.[61] Copper(I) complexes **2a** (0.59 mmol) and **3a** (0.46 mmol) were separately oxygenated at low temperature (–80 °C) in propionitrile. Excess dioxygen was removed by repeated vacuum/argon purging. To confirm that there was no excess O_2, argon was bubbled through the solution; this was passed through the pyrogallol solution. No color change was observed. After 15 min, 2 equiv of PPh_3 was added to the copper dioxygen solution **2c**. Slowly, upon warming the solution from –80 to –65 °C over 3 h, a distinctive change in the color of the pyrogallol test solution from colorless to dark brown indicated the liberation of O_2 from the dioxygen complex **2c**. The same experiment was carried out with the **3b** solution. The same color change was observed for the pyrogallol test solution, except the liberation of dioxygen occurred at relatively higher temperature, e.g. –45 °C. In this case, the temperature was slowly increased from –80 to –45 °C over a 4-h period.

Reaction of Copper Dioxygen Complexes with Triphenylphosphine (PPh_3). Reactions of **2c** and **3b** with PPh_3 were carried out by first applying vacuum/argon to remove any excess of free O_2, followed by the addition of 2 equiv of PPh_3. The reaction mixture was allowed to stir overnight and gradually warm to room temperature. This afforded a light green solution with some blue precipitate. The volume of the solution was reduced by applying vacuum. Diethyl ether (100 mL) was added to the solution to complete the precipitation. The clear supernatant was collected to analyze for the formation of O=PPh_3. The greenhish solid obtained from **2c** was recrystallized from acetronitrile/ether, resulting in a pale yellow powder having the same NMR spectra as the authentic compound **2d-PF_6**, [(BPQA)Cu(PPh_3)]$PF_6 \cdot {}^1/_4Et_2O$ (62% yield). Anal. Calcd for $CuC_{41}H_{37.5}N_4P_2F_6O_{0.25}$: C, 59.29; H, 4.52; N, 6.79. Found: C, 60.05; H, 4.30; N, 7.04. The PPh_3 reaction with **3b** was carried out in a similar manner, giving a pale yellow crystalline material having the same ^{1}H NMR spectrum as the authentic compound **3d-ClO_4**, [(BQPA)Cu(PPh_3)]$PF_6 \cdot {}^1/_4Et_2O$ (58% yield). Anal. Calcd for $CuC_{45}H_{39.5}N_4P_2F_6O_{0.25}$: C, 61.38; H, 4.49; N, 6.37. Found: C, 61.97; H, 4.83; N, 6.23. Gas chromatographic analysis of the ether washings showed that in both cases only a trace amount of O=PPh_3 was present.

Quantitation Determination of H_2O_2: Reaction of $(Cu_n–O_2)^{n+}$ Species with H^+. Typically, copper dioxygen complexes were prepared in situ by bubbling the dry dioxygen gas through a Cu(I)–propionitrile solution (Cu(I) 0.3–0.5 mmol), as described above. Excess O_2 was removed by repeated vacuum/argon purging. Then 5 equiv of $HBF_4 \cdot Et_2O$ (1.5–2.5 mmol) was added to the solution of copper dioxygen complexes. Upon the addition of H^+ at –80 °C, the purple **2c** or brown **3b** solution instantly turned blue. The reaction mixture was stirred for 15 min, followed by the addition of diethyl ether to precipitate a blue Cu(II) product. The precipitate was allowed to settle, and the clear supernatant was transferred with a cannula, to a flask containing a solution of KI (1.0 g) in a degassed mixture of distilled water (20 mL) and acetic acid (10 mL). The blue

precipitate was washed with ether (30 mL) and the supernatant again transferred to the KI solution. The yellow KI mixture was stirred for 15 min at room temperature and then titrated with 0.05 N $Na_2S_2O_3$ solution until it became colorless. The yields of H_2O_2 formed were calculated from the amounts of 0.05 N $Na_2S_2O_3$ consumed: 94% (one trial for **2c**); 89% average (two trials for **3b**).

X-ray Structure Determinations of [(TMQA)Cu]ClO_4 (4a-ClO_4) and [(BQPA)Cu(PPh_3)]ClO_4(3d-ClO_4). A light yellow plate of [(TMQA)-Cu]ClO_4 (**4a-ClO_4**), 0.30 × 0.30 × 0.40 mm, suitable for X-ray diffraction was mounted on a glass fiber. Measurements were made at −20 °C on a Nicolet R3m four-circle automated diffractometer with a Mo X-ray source equipped with a highly ordered graphite monochromator (λ(Mo Kα) = 0.710 73 Å). The structure was solved by direct methods. There are two independent molecules in the asymmetric unit; bond parameters within the two molecules are almost identical. Measurements for the [(BQPA)Cu(PPh_3)]ClO_4 (**3d-ClO_4**) crystal were made on a Rigaku AFC6S diffractometer with a graphite-monochromated Mo Kα source (λ(Mo Kα) = 0.710 69 Å). A light yellow crystal, 0.05 × 0.05 × 0.10 mm, was used, and data collected at room temperature using the ω-scan technique at a scan rate of 4°/min. The structure was solved by direct methods. All non-hydrogen atoms except a few were refined anisotropically. The perchlorate and peripheral carbon atoms of the "dangling" quinolyl group were refined isotropically. A summary of crystal and refinment data for both complexes is provided in Table 1, while Tables 2 and 4 contain positional and equivalent isotropic thermal parameters for **4a-ClO_4** and **3d-ClO_4**, respectively.

Electrochemistry. Cyclic voltammetry and bulk electrolysis were carried out by using a Bioanalytical Systems BAS-100B electrochemistry analyzer connected with a HP-7440A plotter. The cell consisted of a modification of a standard three-chambered design equipped for handling of air-sensitive solutions by utilizing high-vacuum valves (Viton O-ring) seals. Either a platinum disk BAS MF 2013) or a glassy carbon electrode (GCE, BAS MF 2012) was used as the working electrode. The reference electrode was $Ag/AgNO_3$. The measurements were performed at room temperature in DMF solvent containing 0.2 M tetrabutylammonium hexafluorophosphate (TBAHP) and 10^{-3}–10^{-4} M copper complex deoxygenated by bubbling it thoroughly with argon.

Acknowledgment. We thank the National Institutes of Health (Grant GM 28962) for support of this research and the National Science Foundation (Grant CHE-9000471) for help in the purchase of the X-ray diffractometer. We also thank Nepera, Inc., for a donation of the dipicolylamine used in this study.

Supplementary Material Available: Lists of anisotropic thermal parameter and intramolecular bond distances and angles (Tables S1–S6) for **4a-ClO_4** and **3d-ClO_4** (14 pages). Ordering information is given on any current masthead page.